Using Isotopes and Solute Tracers to Infer Groundwater Recharge and Flow in the Cienega Creek Watershed, SE Arizona

USING ISOTOPES AND SOLUTE TRACERS TO INFER GROUNDWATER RECHARGE AND FLOW IN THE CIENEGA CREEK WATERSHED, SE ARIZONA.

by

Rachel S. Tucci

A Thesis Submitted to the Faculty of the

DEPARTMENT OF HYDROLOGY AND ATMOSPHERIC SCIENCES

In Partial Fulfillment of the Requirements

For the Degree of

MASTER OF SCIENCE
WITH A MAJOR IN HYDROLOGY

In the Graduate College

THE UNIVERSITY OF ARIZONA

2018

STATEMENT BY AUTHOR

The thesis titled *Using Isotopes and Solute Tracers to Infer Groundwater Recharge and Flow in the Cienega Creek Watershed, SE Arizona* prepared by *Rachel S. Tucci* has been submitted in partial fulfillment of requirements for a master's degree at the University of Arizona and is deposited in the University Library to be made available to borrowers under rules of the Library.

Brief quotations from this thesis are allowable without special permission, provided that an accurate acknowledgement of the source is made. Requests for permission for extended quotation from or reproduction of this manuscript in whole or in part may be granted by the head of the major department or the Dean of the Graduate College when in his or her judgment the proposed use of the material is in the interests of scholarship. In all other instances, however, permission must be obtained from the author.

SIGNED: *Rachel S. Tucci*

APPROVAL BY THESIS DIRECTOR

This thesis has been approved on the date shown below:

Jennifer McIntosh — *July 27, 2018*

Jennifer McIntosh — Date
Professor of Hydrology

ACKNOWLEDGMENTS

I would like to thank my advisor Dr. Jennifer McIntosh for her patience and willingness to work with me during this journey. I would also like to thank my committee members, Dr. Christopher Eastoe and Dr. Thomas Meixner for their valuable feedback and respected opinions. Additionally, I would like to thank all the residents that allowed me to sample their groundwater wells; without their cooperation this project would not be the same. I would also like to say thank you to Dr. Ron Tiller, Dr. Andrew Salywon, and Erin Gray who helped with sampling in the field and processing in the lab, Kimberly Biesner for showing me how to properly collect groundwater samples for water quality analysis, Floyd Gray for his geologic expertise and Hector Zamora for assistance with cross-section design. A special thank you to Dr. Martha Whitaker who without her endorsement, none of this would have occurred. I would also like to thank Dr. Fred Tillman for his invaluable advice and wisdom, and Tim Corley for showing me how to run the IC and locating my many lab requests. This research was supported in part by The Nature Conservancy, The Bureau of Land Management, and hours of volunteer time by the people previously listed and not listed by name here. Lastly but certainly not least I would like to thank my daughter Violet, husband Jason, and our parents, the Kerrs' and the Tuccis' for their support and belief in me.

TABLE OF CONTENTS

LIST OF FIGURES

LIST OF TABLES

ABSTRACT

The Cienega Creek watershed (CCW) of southern Arizona contains springs and wetlands (cienegas) that support several threatened and endangered species and two registered "Outstanding Arizona Waters" reaches. The lack of baseline scientific hydrologic studies in the CCW leaves important land management questions unanswered, such as how increases in urbanization, ranching, agriculture, or possible mining could impact groundwater resources? To help address these questions, this study investigates the hydrologic connection between recharge in the Santa Rita mountain system and groundwater in basin-fill aquifers, and the source water for the wetlands near Cienega Creek.

Groundwater samples were collected from springs (feeding cienegas), wells, and piezometers completed in basin-fill sediments and shallow alluvial aquifers along a broad transect from the Santa Rita Mountains eastward across the basin to Cienega Creek. Samples were analyzed for major ion chemistry, stable isotopes ($\delta^{18}O$ and δD of water, $\delta^{13}C$ (DIC), $\delta^{34}S_{(SO4)}$ and $\delta^{18}O_{(SO4)}$) and age tracers (^{3}H, ^{14}C). Results indicate springs are dominantly sourced year-round from basin groundwater, and $\delta^{18}O$ values and sulfate to chloride ratios indicate little influence of summer monsoon floodwaters. The low sulfate concentrations and $\delta^{34}S$ values of basin groundwater and springs are typical of local rain water values, and/or indicate small contributions of gypsum dissolution and pyrite oxidation, consistent with the lack of appreciable sulfate sources in basin sediments. Stable water isotopes in groundwater samples across the study area indicate recharge occurred from summer and winter precipitation at approximately 1700 ±200m (mountain front) and higher elevations (mountain block). Most of the groundwater samples analyzed for tritium are below modern precipitation values for the region, and ^{14}C values are low (3.3-84.7 pMC), which indicates most recharge occurred prior to the 1950's, even at the mountain front. The lack of recent recharge in shallow alluvial aquifers beneath the washes and near Cienega Creek suggests that groundwater throughout the basin is a relatively old resource, and future increases in groundwater capture or pumping may impact surface waters, including cienegas.

INTRODUCTION

Groundwater is a particularly important and fragile resource in the semi-arid southwestern United States (US) where groundwater extraction for domestic and municipal consumption, agricultural irrigation, and mining far exceed natural recharge (Baillie et al. 2007; Stonestrom et al. 2007). Increased demands on groundwater supply and projected decreases in recharge due to climate change could threaten this finite resource (Ajami 2009). Climate projections suggest the southwestern United States is expected to become hotter and drier; drought conditions may become more frequent, intense, and longer lasting than in the historical record (Garfin et. al. 2014), which may impact the amount of water available for recharge. A decrease in precipitation could limit mountain system and/or diffuse recharge to basin-fill aquifers, which are the primary groundwater supply for urban areas and agricultural regions in the southwest (Stonestrom et al. 2007; Meixner et al., 2016). Any increases in precipitation and water availability will likely be offset by evapotranspiration due to rising temperatures (Tillman et al. 2011).

The Cienega Creek Watershed (CCW), in southeastern Arizona, contains several federally protected lands, including the Las Cienegas National Conservation Area (LCNCA[1]) in the upper portion of the watershed and the Cienega Creek Natural Preserve (CCNP[2]) in the lower CCW (Figure 1). The CCW also contains two stream reaches, along Cienega Creek and Davidson Canyon, designated as "Outstanding Arizona Waters" under the U.S. Clean Water Act for their superior water quality (A.A.C. R18-11-112(G); PAG 2005). Cienega Creek in the LCNCA flows northward with scattered perennial reaches and a riparian zone corridor along Cienega Creek, which provides connectivity between sky islands of the surrounding mountains (Beier et al. 2007). Wetlands (i.e., cienegas) in the LCNCA flank the upper Cienega Creek and provide important habitat for several threatened and endangered species such as the Huachuca Water Umbel, Gila topminnow, Gila chub, Southwestern willow flycatcher, Chiricahua leopard frog, Mexican garter snake, and Western yellow-billed cuckoo (Federal Register 2014).

An improved understanding of the hydrogeology of the CCW, such as location and timing of groundwater recharge, flow-paths, water residence times, and the degree to which stream reaches and cienegas are dependent on basin groundwater is needed to protect natural resources and assist with future land and water management decisions. This study utilizes chemical and isotopic tracers, together with stratigraphic and piezometric surface information to address the following questions: (1) What is the isotopic composition of precipitation in the CCW, and how does it vary seasonally with altitude? (2) What is the residence time of groundwater? (3) What is the timing and location of recharge in the CCW? And (4) what is the nature of the hydrologic connection between the mountain systems, basin-fill aquifers, and surface waters (springs, cienegas and Cienega Creek)?

Stable water isotopes ($\delta^{18}O$ and δD) were used to evaluate if a seasonal or altitude effect could be identified in precipitation and applied to infer the seasonality and elevation of groundwater recharge across the basin. Radioactive isotopes (^{14}C and ^{3}H) were used to estimate groundwater residence times and identify areas of modern

[1] LCNCA managed by Bureau of Land Management (BLM)
[2] CCNP managed by Pima County Regional Flood Control District (RFCD)

recharge. Sulfate isotopes ($\delta^{34}S$ and $\delta^{18}O$ of SO_4), combined with major ion chemistry, helped identify different sources of solutes (e.g., SO_4, Ca, Na) contributing to groundwater, indicating flow paths of water across the basin and connections to surface water.

BACKGROUND

Study Area and Geology

The CCW is a narrow northwest trending alluvial basin ~965 km^2 in the Basin and Range Province of southern Arizona and ranging in elevation from 975 to 2881m (AZ Water Atlas 2003). This study is focused in the upper CCW on the east side of Santa Rita Mountains and across the basin to upper Cienega Creek in the LCNCA (Figure 1). The study area is bounded by Empire Gulch to the north and Gardner Canyon to the south. Gardner Canyon and Empire Gulch are ephemeral washes that drain southern Arizona's highest peak Mt. Wrightson (elev. 2881m) in the Santa Rita Mountains and are tributaries of Cienega Creek.

The Santa Rita Mountains west of the study area are mostly Mesozoic volcanic and sedimentary rocks composed of Triassic volcanics seen in the Mount Wrightson and Gardner Canyon formations and Early and Late Cretaceous sandstone, siltstone, and conglomerates seen in the Bisbee and Salero formations (Drewes 1971). Most of the Santa Rita Mountains are "abundantly faulted and less commonly folded," however the central structural unit, apart from two major fault zones, is slightly faulted with extensive folding (Drewes 1972). Large northwest trending fault zones (Sawmill Canyon and Big Casa Blanca Canyon) cut orthogonal to Gardner Canyon at the range front (Drewes 1972; plate 1). The region between the fault zones, Adobe Canyon structural block, is strongly folded with little faulting (Drewes 1968). The Big Casa Blanca Canyon fault and the nearby subparallel Sawmill Canyon fault zone were active intermittently from the Paleocene to the middle Oligocene and were formed as a result of northeast to southwest oriented compression (Drewes 1981). Dikes of the Gardner Canyon swarm are thought to be Oligocene in age (Drewes 1972).

The northern boundary of the study area is underlain by Late Cretaceous sedimentary sandstone, conglomerates and gray marine limestone strata that dip southward. Tertiary conglomerate and sandstone (Pantano Formation) were deposited on top of the Cretaceous strata during late Oligocene and early Miocene faulting and make up the lower basin-fill unit (Bittson 1976). Outcrops of the Pantano Formation in the southwest Tucson Basin are highly faulted and tilted (Anderson 1987). The Pantano Formation in the lower CCW is approximately 1830m thick and the stratigraphic facies are described as fanglomerates, mudflow units and volcanics (Cohee et al. 1976). These units consist of heterogenous unconsolidated to consolidated sedimentary rocks (Bittson 1976). A distinction between basin-fill deposits and Pantano Formation in the study area cannot be well defined because they contain similar lithology, but different geologic structures that cannot be seen in the well logs; correlation of units in the lower CCW and the study area is not advised (Gray, personal communication 2018). Pleistocene and Holocene basin-fill deposits can be 610m deep in the Tucson area and are considered unconsolidated gravels, landslide debris and alluvium (Drewes 1972; Bittson 1976). Surficial quaternary deposits found in the lower valley region of the LCNCA can be up to 90m and consist of sand and gravel (Drewes 1972; Stonestrom et al. 2007).

The main sources of sulfate in the semi-arid Basin and Range Province of southern Arizona are Permian marine gypsum and igneous sulfide commonly derived from Laramide granitoids, volcanic rock, and meteoric sulfate in precipitation and dust (Gu et al. 2008). Previous studies in the region have shown that sources of sulfate (i.e., pyrite oxidation, gypsum dissolution, rainwater) in natural waters have different isotopic signatures (Gu 2005). In the adjacent Sonoita Creek three different sulfate sources can be identified; reworked Permian marine gypsum in the Pantano Formation from surrounding mountains, acid rock drainage from previous mining, and rainwater (Gu et al. 2008). The dominant source of sulfate in the Tucson Basin is Permian marine gypsum with distinct sulfur isotope signatures from the surrounding mountain ranges transported to the basin floor through washes draining the higher mountain elevations (Eastoe et al. 2004; Gu 2005).

Hydrogeology

The primary CCW aquifer(s) are in water-bearing units of unconsolidated stream alluvium, semi-consolidated upper basin-fill, and Tertiary indurated lower basin-fill of the Pantano Formation, which overlies the Upper Cretaceous carbonate aquifer (Huth 1996, Coes and Pool 2007). For this study the aquifers are defined as the shallow basin-fill aquifer, which extends through the upper basin-fill and the deeper regional aquifer is in the lower basin-fill (Tertiary Pantano Formation) and Upper Cretaceous unit. Previous studies have not defined whether there are two aquifers separated by an aquitard or if there is one large continuous aquifer.

The unconsolidated Quaternary alluvium deposited around Cienega Creek has a transmissivity range of 124 to 621 m^2/d based on pumping tests (Harshbarger and Assoc. 1975). The semi-consolidated upper basin-fill aquifer transmissivity ranges from 6 to 62 m^2/d (Harshbarger and Assoc. 1975). The Tertiary lower basin-fill aquifer has very low transmissivities, although actual values were not reported (Huth 1996). The total storage for CCW to a depth of 366m has been estimated as 6291 to 13,569 million m^3 (AZ Water Atlas 2010). Typical Basin and Range basin-fill aquifers have hydraulic conductivities ranging from 0.0007 to 43m/d, dependent on lithology and the occurrence of faults or fractures in water bearing units (Stonestrom et al. 2007). Previous consultant studies in the area estimate recharge rates along the Santa Rita mountain front range from 10,665 to 20,263 m^3/day (Harshbarger and Assoc.1974; Rosemont Copper Co. 2012).

Groundwater supply in the Basin and Range aquifers is reliant on four main recharge mechanisms including mountain block and mountain front recharge, together comprising ‘mountain system’ recharge (Stonestrom et al. 2007; Meixner et al. 2016), incidental diffuse recharge, and ephemeral channel recharge (Phillips et al. 2004). The same four mechanisms are expected in the upper CCW; (1) mountain-block recharge from high elevation carbonate aquifers; (2) mountain-front recharge from streams and runoff that cross the mountain-range front; (3) diffuse recharge between major washes in the basin-fill deposits; and (4) ephemeral channel recharge along Gardner Canyon, Empire Gulch, and Cienega Creek (Eastoe et al. 2004; Stonestrom et al. 2007).

The water level surface map (Figure 2) across the study area implies that the direction of groundwater flow is from the mountain system east-northeast across the study area (Huth 1996). A groundwater divide south and east of the study area separates the CCW from the Sonoita Creek and Babocomari (San Pedro) watersheds. (Huth 1996; Boggs 1980).

Previous hydrogeochemical models across the study area noted a difference in major ion chemistry between the shallow basin-fill aquifer and the deeper regional aquifer. Groundwater chemically evolves from Ca-Mg-HCO_3 type waters at the Santa Rita mountain front to Na-HCO_3 type waters in the central basin, suggesting the importance of cation exchange on water chemistry; however, a continuous clay layer could not be identified in available driller's logs at the time (Harshbarger and Assoc. 1975; Huth 1996). In the adjacent Sonoita Creek Basin to the southwest, baseflow to Sonoita Creek is dominated by Ca-HCO_3-SO_4 type waters (Gu et al. 2008). Lower Cienega Creek surface waters are Na-Mg-SO_4 type waters with high sulfate concentrations unlike the more dilute, Ca-HCO_3 type waters found in springs and wells near the upper reaches of Cienega Creek (Pima Association of Governments, 2000). Previous studies in the adjacent middle San Pedro basin to the east, demonstrated the importance of high-elevation mountain system recharge consisting of winter precipitation to the basin-fill aquifer (Baillie et al. 2007; Wahi et al. 2008; and Hopkins et al. 2014) and showed that the presence of clay confining units increased groundwater residence times in the lower basin-fill aquifer (Hopkins et al. 2014).

The Santa Rita Mountains are rich in mineral resources (Drewes 1973) and have been mined intermittently since the 18th century (Schrader 1915). Since the 1970s various companies have shown interest in re-establishing mining for copper in the northern Santa Rita Mountains, north of the upper CCW. Three comprehensive hydrologic models have been recently constructed for the proposed Rosemont open-pit copper mine. The models developed by Montgomery & Associates (M&A) and Tetra Tech (TT) include Cienega Creek in the LCNCA and Davidson Canyon north of the study area, while the Water & Earth Technologies, Inc. (W&ET) model focused only on Davidson Canyon. An Integrated Watershed Summary produced by Rosemont Copper Co. found that mountain precipitation enters the CCW and recharges groundwater through fractured bedrock and basin-fill (M&A and TT). Most of the water leaves the CCW groundwater system through evapotranspiration, and there is minimal discharge from springs to streams (M&A and TT). Reports suggest that north of the study area, the geology is complex with variable fracture densities and isolated faults with limited hydraulic connectivity (M&A and TT), indicating results may vary based on the different geologic stratigraphy and structures throughout the watershed.

Climate

The timing and areal distribution of precipitation affect recharge rates in alluvial basin aquifers (Coes and Pool 2007). Southern Arizona has two rainy seasons, summer and winter, with largest precipitation occurring in July-August and November-March. Precipitation is most likely to recharge the aquifer during the wettest months- probably the wettest 30% of months, on the basis of stable isotope data (Figure 3; Eastoe and Towne 2018) because the quantity of water is large enough to infiltrate through the vadose zone and reach the water table through washes and highly permeable soil zones that have increased hydraulic conductivities. The other 70% of precipitation months have lower precipitation intensity, thus precipitation is likely returned to the atmosphere via evapotranspiration (ET) processes and does not infiltrate to the water table (Jasechko and Taylor 2015; Eastoe and Towne 2018).

The average precipitation across the CCW ranges from 41cm in lowlands to 102cm in the mountains (AZ Water Atlas 2003). Summer monsoons are responsible for approximately 65% of the annual precipitation, while winter precipitation accounts for ~35% (Huth 1996). Previous stable isotope studies of ground water in adjacent alluvial basins found winter precipitation is a more important source of recharge than summer precipitation (Eastoe et al. 2004; Baillie et al. 2007; Ajami 2009); mountain system recharge has a 65% ± 25% contribution from winter precipitation and a 35% ± 25% contribution from summer precipitation (Wahi et al. 2008). Research in the middle San Pedro Basin concluded that groundwater with relatively low $\delta^{18}O$ values was recharged from winter precipitation, with no detectable isotope effects of evaporation or water-rock exchange (Hopkins et al. 2014). Tucson groundwater samples plot close to the local meteoric water line (LMWL), which also indicate minimal evaporation during recharge (Eastoe et al. 2004). Recharge rates during the late Pleistocene pluvial periods were higher than at present in southern Arizona due to wetter and cooler climatic conditions (Stonestrom et al. 2007).

Vegetation

Grasslands in the Sonoran Desert have been stable for thousands of years, however the composition of species varied continuously in response to changing climates (McClaran and Van Devender 1995). Grasslands of North America cannot confidently be traced by the fossil record beyond 11,000 years ago (McClaran and Van Devender 1995). The current upper CCW is covered by various types of vegetation including “plains, great basin, and semi-desert grasslands, Chihuahuan desert scrub, and madrean evergreen woodland and a small portion of Rocky Mountain and montane madrean conifer forest” (AZ Water Atlas 2003). Non-native flora, intentionally planted as forage for livestock and erosion prevention on rangelands along Cienega Creek, started at the turn of the twentieth century with Bermuda grass, then later in the 1930’s with Lehmann Lovegrass, which now dominates the upper elevation grasslands of southern Arizona, and an increase of shrub and succulent communities across the landscape have occurred, where more biodiverse grasses used to thrive (McClaran and Van Devender 1995).

METHODS

Water samples were collected from wells, piezometers, springs, cienegas and precipitation collectors in the upper CCW from April 2014 through June 2017. Well, piezometer and spring samples were primarily collected along the washes that drain the eastern side of the Santa Rita Mountains and are tributaries of the upper reaches of Cienega Creek in the LCNCA. All groundwater samples were analyzed for water stable isotopes ($\delta^{18}O$ and δD) and major ion chemistry. Selected samples were analyzed for solute isotopes ($\delta^{13}C$–DIC, $\delta^{34}S$-SO_4, $\delta^{18}O$-SO_4) and age tracers (^{14}C and ^{3}H). Precipitation samples were analyzed for water stable isotopes ($\delta^{18}O$ and δD). In addition, previous chemical and isotopic data from the CCW and Sonoita Creek Basin were incorporated into this study for comparison (Regional Flood Control District of Pima County; Geraghty & Miller Inc. 1970; Harshbarger and Assoc. 1974; Eastoe et. al. 2004; Sky Island Alliance and Final Environmental Impact Statement submitted by Hudbay Minerals Inc. 2014; Truebe 2016) (Appendix A).

Forty-two samples were collected from domestic wells across the study area and exploratory mining wells in the LCNCA. Static water levels, reported in well logs, ranged from 45 to 390m below ground level. Well latitude, longitude and surface elevation were recorded with a Global Positioning System Garmin eTrex 10® (Table 1). One end of a garden hose was attached to a hose bib and the other end connected to a flow through chamber with inserted temperature, pH, electric conductivity, and dissolved oxygen sensors of a Fisher Scientific Orion 5 Star meter (Table 2). The faucet was then turned on and once the parameters had stabilized and were recorded, the samples were collected. Water samples were filtered using a 0.45-μm nylon filter in a Nalgene reusable filter housing, pre-rinsed with filtered sample water. Sample aliquots for $\delta^{18}O$ and δD were collected in glass scintillation vials with a poly seal cone cap and no head space. Aliquots for alkalinity and anions were collected in HDPE bottles with no head space, while cation samples were collected in acid-washed HDPE bottles and preserved with optima-grade concentrated nitric acid. Aliquots for $\delta^{13}C$-DIC were collected in glass serum bottles with crimp top caps and no head space. Samples were placed on ice, returned to the lab and stored in a refrigerator at 4°C until analyzed. Unfiltered samples for tritium and sulfur isotope measurement were collected in 1 liter HDPE white and amber bottles, respectively, direct from the faucet. Each bottle was rinsed with sample water 3 times before filling with no head space. Sulfur isotope samples were preserved with 10 drops of concentrated nitric acid to prevent bacterial sulfate reduction. Sample bottles were sealed with black electrical tape and placed on ice until returned to the lab where the sulfur isotope samples were stored in a refrigerator at 4°C and the tritium samples were stored at room temperature. Unfiltered sample aliquots for ^{14}C and $\delta^{13}C$-DIC were collected directly from the faucet in a 1 liter amber glass bottle with a silicon tube inserted into the faucet and the other end in the bottom of the bottle to fill without head space and air bubbles. Sample lids were sealed with black electrical tape and placed on ice until returned to the laboratory where they were stored at 4°C prior to analysis.

Nine piezometer and fifteen spring samples in the LCNCA were collected in two 125ml HDPE clear bottles, one acid washed with nitric-acid, and one washed with DI water. The samples were kept on ice until they were brought back to the laboratory and refrigerated before filtering. Samples were filtered through a 0.45-μm nylon filter in a Nalgene reusable filter housing. Filtered sample water from non-acid washed bottles were poured into clear 30mL HDPE bottles with no headspace for anion and alkalinity analysis. Filtered sample water from acid washed bottles were poured into clear 30 mL HDPE bottles with no headspace and 2 drops of nitric acid were added to preserve for cation analysis. Unfiltered tritium and sulfur isotope samples were collected from selected sites in 1L HDPE clear and brown bottles, respectively. Because of the heavy sediment and organic matter load in the spring and piezometer water samples, tritium and sulfur isotope aliquots for these samples were filtered through lint-free 100% cotton cheese cloth and nylon stockings prior to analysis.

Twelve precipitation collectors were setup along an elevation gradient (1070 to 2615m) across the CCW (Figure 1). Five-gallon buckets were deployed prior to the wet season with mineral oil to minimize evaporation and samples were collected twice a year in late spring following the wet winter season and early fall following the summer monsoon season. The water was sampled by inserting a plastic tube into the bucket connected to a syringe on one end and rinsing out the syringe three times before taking the sample. Unfiltered $\delta^{18}O$ and δD samples were collected in clear 30ml glass bottles with a poly seal cone cap with no head space. Precipitation samples were analyzed for stable water isotopes. All analytical methods, precision, and laboratories where the analyses were conducted are summarized in Table 3.

RESULTS

Precipitation Stable Water Isotopes

The isotopic composition of precipitation was investigated across an elevation gradient in the CCW (Figure 4; A and B). Precipitation samples from this study were compared to the long term (30-year) averages collected in the Tucson Basin and Santa Catalina Mountains, north of Tucson, Arizona. The trend lines for summer and winter precipitation shown in Figure 4, represent seasonal mean $\delta^{18}O$ values for summer and winter precipitation collected in the adjacent Tucson Basin and Palisades Ranger station in the Santa Catalina Mountains from 1981 to 2015 (Wright 2001; Eastoe et al. 2004). The highest elevation in the study area (Mt. Wrightson in the Santa Rita Mountains) is higher than available data for the Santa Catalina Mountains. Unlike long term (30-year) precipitation records in the Tucson Basin (Wright 2001; Eastoe et al. 2004; Eastoe and Dettman 2016), precipitation samples in this study (2015-2017) do not show differences with elevation over the 2-year study period.

The Tucson Basin mean $\delta^{18}O$ and δD values for summer and winter precipitation are shown for high elevations with closed solid green symbols (2420m; (-8.6‰, -56‰) and (-10.9‰, -70‰), respectively) and low elevations with solid purple symbols (1700m; (-7.5‰, -51‰) and (-10.1‰, -64‰), respectively) in Figure 5 A and B. Mountain front elevations in the study area are ~1700 ±200m. Precipitation samples collected as part of this study, have $\delta^{18}O$ values ranging from -12.5 to 0.8‰ for summer and -13.9 to -2.4‰ for winter, and δD values ranging from -88 to 7‰ for summer and -91 to -4‰ for winter (Table 4). These are consistent with the precipitation values previously reported by Hudbay Minerals Inc. (FEIS 2013) collected north of the study area in 2012-2013 (Appendix A).

In Figure 5A summer precipitation samples plot around the expected weighted average for winter and the winter precipitation samples plot around the expected weighted average for summer seen in the Santa Catalina Mountains (Eastoe and Dettman 2016). The winter precipitation sample for PT1 is enriched in ^{18}O and appears significantly evaporated. Summer precipitation samples with little evaporation in Figure 5B plot around the expected summer weighted average for the Tucson Basin based on long term data for Tucson (Eastoe and Dettman 2016). Winter precipitation samples do not plot around the expected weighted mean for Tucson winter precipitation, rather they cluster about the expected mean for summer. Evaporation effects can be seen for both the summer and winter precipitation samples for the study area; the evaporation trend in Figure 5B has a slope of 4.

Stable Isotopes of Water in Groundwater

Two types of LMWLs are shown on Figure 6: (1) the LMWL for 1700m, representing all precipitation, is drawn through long term amount-weighted summer and winter mean $\delta^{18}O$ and δD values [(-7.5‰, -51‰) and (-10.1‰, -64‰), respectively]; (2) a modified LMWL for 1700m is drawn through points representing amount-weighted means for the wettest 30% of months in summer and winter [(-7.7‰ $\delta^{18}O$, -52‰ δD) and (-10.6‰ $\delta^{18}O$, -74‰ δD), respectively]. This type of modified LMWL is thought to be more representative of recharge processes at altitudes where direct runoff of rainwater leads to recharge (Jasechko and Taylor 2015; Eastoe and Towne 2018). The summer and winter points are derived from Tucson Basin data (Figure 3), with altitude corrections. The 1700m (30% wettest) LMWL plots near the GMWL with a slope of 7.7, whereas the 1700m (all months) LMWL plots above the GMWL with a slope of 4.8.

At high altitudes, where snowpacks accumulate in winter, winter recharge is likely to reflect all winter precipitation (because meltwater represents the whole snowpack), while summer recharge is most probable from runoff in the wettest 30% of summer months (Jasechko and Taylor 2015; Eastoe and Towne 2018). Therefore, for 2420/2600m elevation, the amount-weighted winter mean represents precipitation from all months and [(-11.1‰, -72‰), 2600m only), while the summer mean represents only the wettest 30% of months [(-9.5‰, -62‰) and (-8.9‰, -57‰), respectively]. The 2600m (all months) LMWL, plots above the GMWL with a slope of 6.5.

The isotopic composition of water samples from wells, piezometer, and springs were plotted in relation to the LMWLs described in Figure 6 to determine if the altitude or seasonality of groundwater recharge could be evaluated with the current dataset (Table 4). There is significant overlap of $\delta^{18}O$ (-5.0 to -12.4‰) versus δD (-44 to -81‰) values between the different water types (wells vs springs), and most of the samples plot to the right of the LMWLs. The 2600m (all months) LMWL, plots above the GMWL with a slope of 6.5. The high elevation spring samples plot near and above the 2600m (all months) LMWL. Certain well, piezometer, and spring samples plot near and above the 2600m (all months) LMWL. A group of data (wells, piezometers and lower elevation springs) plot near the 1700m (30% wettest) LMWL between the summer and winter mean precipitation values from the long term Tucson Basin record (Eastoe and Dettman, 2016). The remaining samples plot below the 1700m (30% wettest) LMWL, with some samples highly enriched in ^{18}O, above the mean summer precipitation value for Tucson.

Sulfur and oxygen isotopes of sulfate in groundwater

The range of $\delta^{34}S_{(SO4)}$ and $\delta^{18}O_{(SO4)}$ values for different potential sulfate sources to groundwater, previously identified in adjacent basins (Gu 2005), is indicated by the black dotted fields in Figure 7. The fields for pyrite oxidation and gypsum dissolution were created from groundwater samples in the adjacent Sonoita Creek area and the field for sulfate in precipitation (rain and snow) comes from Tucson Basin precipitation (Gu et al. 2008). The majority of water samples in this study have $\delta^{34}S_{(SO4)}$ values ranging from +2.8 to +10.7‰ and $\delta^{18}O_{(SO4)}$ values ranging from +2.8 to +13.7‰ (Table 4). Most of the water samples collected in this study plot outside the previous values for the Sonoita Creek area and Tucson Basin. Wells (WL13 and WL14) and SP1, at the Santa Rita mountain front, have elevated $\delta^{34}S_{(SO4)}$ values closer to the $\delta^{34}S_{(SO4)}$ value measured in a speleothem sample from the Cave of the Bells (11.3‰; Gu 2005). Two piezometers (WP-2 and WP-14) plot as outliers with $\delta^{18}O_{(SO4)}$ values of -5.4 and +26.0‰, respectively.

Sulfur isotope values were plotted against $1/SO_4^{2-}$ to emphasize the low sulfate concentrations measured in the majority of water samples in the study area (Figure 8). Sulfate concentrations range from 6.20 to 390 mg/L; with the majority having less than 29.46 mg/L SO_4^{2-} (Table 5). Most of the groundwater samples, Cave of the Bells and Onyx Cave drip water samples (4.3‰ and 3.9‰, respectively) have $\delta^{34}S_{(SO4)}$ values within the range of atmospheric $\delta^{34}S_{(SO4)}$ (+2.1 to +8.0‰) for the Tucson Basin (Gu 2005) (Figure 8). Two piezometer samples (WP07 and WP14) have $\delta^{34}S_{(SO4)}$ values (-1.1 and -5.2‰, respectively) similar to the reported range for pyrite oxidation in the Sonoita Creek area (Gu 2005). Most mountain front and some LCNCA groundwater samples have $\delta^{34}S_{(SO4)}$ values in the range of gypsum dissolution (Gu 2005).

SO_4^{2-}/Cl^- Ratios in Groundwater

Most of the water samples collected in this study have low sulfate to chloride mass ratios (0.41 to 19.11) similar to the range of mass ratios reported for Tucson Basin rainwater (0.9 to 7.8; Gu 2005) (Figure 9; Table 5). The highest SO_4^{2-}/Cl^- mass ratio (101.05) was measured in a piezometer (PZ6) in the LCNCA (not shown in Figure 9). PZ6 is located on the northwest corner of an old agricultural field along the eastern side of Cienega Creek. Groundwater and surface waters with higher sulfate to chloride ratios have been observed in the adjacent San Pedro and Sonoita Creek watersheds up to 74.3 (Hopkins et al. 2014) and 51.17 (Gu 2005), respectively and in the lower CCW up to 45.35 (Appendix A).

Ca^{2+}/Na^+ Ratios in Groundwater

Calcium to sodium mass ratios for the study area range from 0.02 to 11.51 (Figure 10; Table 5). Groundwaters at the mountain front (SP1, WL13, and WL14) have Ca^{2+}/Na^+ values of 11.51, 10.55, and 7.97, respectively. Two groundwater samples along Garden Canyon (WL15 and WL37) have Ca^{2+}/Na^+ values of 7.01 and 7.00, respectively. Most samples away from the Santa Rita mountain front to Cienega Creek in the LCNCA have Ca^{2+}/Na^+ values ranging from 0.02 to 5.73. One LCNCA spring sample (SP4), out of the 3 times measured, has a Ca^{2+}/Na^+ mass ratio of 10.27, which is larger than the range of samples found across the basin.

Tritium and ^{14}C Groundwater Residence Time

Eleven of the groundwater samples measured in this study contain low, but detectable tritium, while 23 samples have tritium below the detection limit (<0.5 tritium units (TU)) (Figure 11A; Table 4). Tritium values range from below the detection limit (<0.5TU) to 2TU, less than the range of amount-weighted annual mean tritium in precipitation measured from 1970 to 2017 in the Tucson Basin (3.1 to 5.3TU; Eastoe et al. 2011; Eastoe, pers. comm. 2017).

The spatial distribution of tritium values measured in samples from wells, piezometers, and springs across the study area is shown in Figure 11B. Detectable, but low tritium (>0.5 to 1.9 TU) was measured in well, spring and piezometer samples along the Gardner Canyon and Empire Gulch washes, Cienega Creek, and at the mountain front (wells and a spring). Most of the samples across the study area do not contain detectable tritium (Figure 11B).

Radiocarbon (^{14}C) values range from 3.3 to 84.7 percent modern carbon (pMC) (Figure 12 A and B; Table 4), with unadjusted ages ranging from 28,000 to 1,300 years old, respectively, using the radioactive decay equation with q equal to 1 and the initial ^{14}C ($a_o{}^{14}C$) equal to 100 pMC. The radioactive decay equation is defined as $t = -8267 * \ln\left(\frac{a_t{}^{14}C}{q * a_o{}^{14}C}\right)$, t is equal to 'age', a_t is equal to the activity of the ^{14}C measured in DIC, a_o is equal to the initial activity of the ^{14}C in DIC, and q is the dilution factor (Clark and Fritz 1997). Adjusted ages were calculated assuming q equal to 0.85, which is the highest ^{14}C value measured in this study at the Santa Rita mountain front in a well with measurable, but near detection limit tritium (WL13, 84.7 pMC). Adjusted ages represent maximum travel times of groundwater from the Santa Rita mountain front to wells downgradient, not accounting for carbonate dissolution.

The lowest ^{14}C values (3.3 to 13.6 pMC) were found in groundwater from deep (258 to 392m depth) mining exploratory wells drilled in the LCNCA in the 1970's with adjusted ages ranging from 27,000 to 15,000 years old. SP10, located in the LCNCA, contains 75.8 pMC with an adjusted age of ~1000 years. The altitude of SP10 shown in (Figure 12A) is the point on the land surface where the sample was collected and corresponds to the same altitude as the well depths measured for ^{14}C across the study area. The spatial distribution of ^{14}C values measured in samples from wells across the study area and SP10 is shown in Figure 12B. Groundwater samples measured in wells less than 143m deep, close to washes, and SP10 contain >58.9 pMC ^{14}C and the adjusted ages range from 30 to 3,000 years.

DISCUSSION

Highly Variable Stable Isotope Composition of Precipitation

Stable water isotope values of local precipitation collected in the CCW, measured over the course of 3 years by Hudbay Minerals Inc. and this study (Dec 2012- Aug 2013 and Nov 2015- Dec 2017), do not show an altitude effect for seasonal precipitation (Figure 4 A and B). A seasonality effect consistent with long term observations in Tucson, where average $\delta^{18}O$ and δD in winter are lower than in summer (Eastoe and Dettman 2016) could be seen with the low elevation 2013 data; however, it could not be seen in the 2015-2017 precipitation data (Figure 4B). During this period, average $\delta^{18}O$ and δD values of winter precipitation are either approximately the same, or greater than summer averages. This is consistent with recent trends seen in the adjacent Tucson Basin record since 2014, during which time winter and summer averages have been similar (Eastoe and Towne 2018).

The lack of discernible trends in precipitation stable isotope values with altitude or seasonality in this study may be due to a change in moisture sources for precipitation in the region over the relatively short sampling period. Reversals of the expected seasonal relationship ($\delta^{18}O$ and δD lower in winter than in summer) have been observed at high altitude in the study area, between 2015 and 2017 (Figure 4A). Summer precipitation values may have been affected by active hurricane seasons that moved over the region lowering $\delta^{18}O$ values to resemble winter or high elevation precipitation (Eastoe 2016; Eastoe and Dettman 2016). A longer record, such as available for the Tucson Basin (Eastoe and Dettman 2016), is needed to characterize local precipitation stable isotope values for recharge to groundwater with residence times greater than a few years. The anomalous precipitation years are important for understanding the isotopic composition of young groundwater, resident for a few years. Such groundwater may be identified in future studies.

Old Groundwater Throughout the Study Area

Most groundwater across the study area is older than 70 years based on tritium values below detection limit (<0.5 TU), and relatively low ^{14}C values (Figure 11B and 12B). The few samples with detectable tritium had low values (<2 TU) which indicate a mixture of older and modern water recharge with a larger older water component. The youngest water is found at the mountain front and the oldest water (3.3 to 13.6 pMC; 15,100 to 26,800 adjusted ^{14}C ages) is found in the deepest wells (>258m deep) in the LCNCA. Radiocarbon values ≥50 pMC, corresponding to unadjusted ages of ≤5700 years, are common in the adjacent San Pedro, Patagonia, and Tucson basins along washes and creeks (Eastoe 2004; Gu 2005; Hopkins et al. 2014). The majority of wells and SP10 have ^{14}C values ranging from 77.1 to 58.9pMC (with adjusted ages of 800 to 3,000 years old, respectively), and appear to come from a similar shallow basin-fill aquifer based on the similar altitudes of the static water levels (~1440m). The addition of dead carbon from carbonate dissolution was not accounted for in the calculation of adjusted ages. The $\delta^{13}C_{DIC}$ values in groundwater range from -13.1 to -5.9‰ (Table 4), indicating some addition of DIC from carbonate dissolution. Accounting for such additions would decrease the actual groundwater ages by hundreds to thousands of years.

Low $\delta^{18}O$, Tritium, and Sulfate Values Reveal Recharge Location and Source

In the Basin and Range aquifer systems, like the Santa Rita Mountains, mountain front recharge is expected to be a larger contributor than mountain block recharge to groundwater, partially due to the larger surface area when compared to high elevation mountain tops (Osterkamp 1973; Stonestrom et al. 2007; Meixner et al. 2016). In the upper CCW the mountain front elevation is at 1600 ±200m and the mountain block is ≥1800 ±200m. Whether the groundwater recharged at the Santa Rita mountain front (~1700 ±200m) during the summer and winter and/or at higher elevation (~2600m ±200m) is less certain based on the groundwater samples that plot around both LMWLs in Figure 6.

Most of the array of groundwater samples could be formed by either evaporation of water recharged at high-elevations, like seen in the high-elevation springs of the Santa Rita Mountains, or by evaporation of water that infiltrated from precipitation that fell near the range front (1700 ±200 m). The clustering of data points along the LMWL for 1700 m suggests that infiltration at that altitude may be predominant. In addition, the geometry of the Santa Rita Mountain range, with less surface area at high-elevations and more surface area near the base (mountain front), suggests that infiltration near 1700m is more likely than at mountain summits. Considering clustering of data along the 1700 m LMWL, some samples show mainly summer recharge, while others show about equal summer and winter recharge.

Groundwater samples that plot above all LMWLs and the GMWL, enriched in ^{2}H and have low $\delta^{18}O$ values (<-9‰) were likely recharged by winter precipitation at high elevations and may be due to contributions of isotopically enriched snow melt (Clark and Fritz 1997). Additionally, some recharge appears to have occurred in the geologic past under cooler and wetter climatic conditions based on their relatively low $\delta^{18}O$ and δD values and groundwater residence times around the middle Holocene. Average $\delta^{18}O$ values of precipitation in Cave of the Bells collected from speleothem samples, were ~2.5‰ lower in the Late Pleistocene/ Early Holocene (14,000-15,000 years ago; Wagner et al. 2010) when recharge rates were higher compared to the present (Stonestrom et al. 2007). Pollen collected from alluvium in southeastern Arizona dating to the middle Holocene (4,000+ year ago) indicate summer monsoon seasons were stronger than those of today and evidence of perennial water can be seen in playas in New Mexico, which indicate wetter conditions 12,000 to 4,000 years ago and again 3,000 to 1,000 years ago (McClaran and Van Devender 1995).

The spring (SP1) and well (WL13) sampled at the Santa Rita mountain front contained low, but detectable tritium (0.9 and 0.8 TU, respectively), indicating a mix of mostly older and some modern water, suggesting minimal and/or slow-moving modern mountain front recharge. An additional well (WL38), also at the mountain front contained below detectable tritium, indicating no modern recharge. Washes (Gardner Canyon, Cave Creek, and Fish Canyon) at the mountain front are observed to flow after summer monsoon flood events and during spring snowmelt, however the surface runoff does not appear to be a large contributor to groundwater sampled for this study. This is in contrast to what has been observed in the lower Cienega Creek and adjacent San Pedro and Tucson basins where modern recharge tritium values (3.1-5.3 TU) (and post-bomb ^{14}C) are seen in groundwater near washes, ephemeral creeks and at the mountain front (Eastoe et al. 2004; Wahi et al. 2007; Hopkins et al. 2014). There were, however, no shallow piezometers adjacent to Gardner Canyon and Fish Canyon near the mountain front; thus we cannot rule out focused recharge of recent runoff at the base of the Santa Rita Mountains where additional work is needed.

The lack of modern recharge or slow-moving recharge observed at the Santa Rita mountain front in the study area may be a result of the Big Casa Blanca Canyon fault and Sawmill Canyon fault zone. The fault zones, which trend northwest or southeast could cause modern recharge to take preferential flow paths by-passing the study area. Two limestone caves in the fault zones, Onyx and Cave of the Bells, are surrounded by “insoluble” (impermeable) sandstone, and their formation has been attributed to extremely slow-moving groundwater (Brod 2005). Groundwater may slowly enter the study area through fractures orthogonal to the northwest or southeast trending fault zones or deep flow paths of high altitude recharge that moves through the mountain block, under the large fault zone and into the regional aquifer. Additional geochemical data would need to be collected to further understanding of the fault zones impact on recharge to the upper Cienega Creek Watershed.

Modern, focused recharge was also anticipated along Gardner Canyon and ephemeral washes out in the basin like Empire Gulch, similar to what has been observed in surrounding watersheds (Eastoe et al. 2004; Hopkins et al 2013). Unexpectedly, samples collected from wells along Gardner Canyon, > 8.5km from the mountain front, and springs and piezometers along Empire Gulch, and Cienega Creek in the LCNCA had detectable, but low tritium values (0.8 to 1.9 TU), which indicate a mixture of mostly older and some modern water, similar to what was seen at the mountain front. Two wells sampled along Gardner Canyon (WL11; 1.7TU and WL15; 2TU) with low detectable tritium values were located near manmade stock-ponds, which provide a possible location for modern precipitation to infiltrate to the aquifer.

Results from this study confirm that recent and diffuse recharge is limited across the study area, in part because the landscape is dominated by grasslands which increase evapotranspiration and have large impacts on available water as it moves through the root zones (AZ Water Atlas 2010; Glenn et al. 2015). Infiltration of rainwater within the central basin grasslands is assumed to be negligible based on previous studies (Huth 1996). Water stable isotope results from this study also suggest groundwater recharge occurred at the mountain front and/or at higher elevations through the mountain block. Tritium values close to detection limit (<0.5 TU) and relatively low radiocarbon values (<84.7 pMC) show widespread pre-bomb (pre-1950’s) recharge across the basin in all sampling locations. Older water found in adjacent basins was located in the central parts of basins, remote from major water courses and mountain fronts (Eastoe et al. 2004; Hopkins et al. 2014). Similar trends were observed in this study area.

The low sulfate concentrations and $\delta^{34}S$ values of groundwater samples, within the range of local precipitation (Gu 2005), may suggest most of the sulfate in the groundwater in the study area came from atmospheric sources with limited addition of sulfate from rock derived sulfur, which is consistent with the sulfur-poor composition of the basin sediments. Alternatively, there could be some mixing of sulfate from pyrite oxidation and gypsum dissolution, in addition to atmospheric sources, as most of the groundwater samples plot between the three fields in Figure 7 in terms of their $\delta^{18}O$ and $\delta^{34}S$ values of SO_4.

Springs that supply water to the cienegas surrounding Cienega Creek in the LCNCA appear to be sustained by the basin-fill aquifer based on similar sulfate to chloride mass ratios, and relatively long residence times (<84.7 pMC and <1.9 TU). Spring and well samples in this study have similar sulfate to chloride mass ratios as Tucson Basin groundwater (Gu 2005).

Non-Atmospheric Sulfur Isotopes Explained

Two piezometer samples had a sulfur isotope signature indicating pyrite oxidation, similar to what was found in the Sonoita Creek Basin (Gu 2005). Piezometer sample (PZ4) had a $\delta^{34}S_{(SO4)}$ value in the range of pyrite oxidation and low dissolved oxygen (7.4%), which may be indicative of a phase of bacteria sulfate reduction and sulfide formation, followed by sulfide oxidation. In the dark organic rich sediments characteristics of the Oak Tree canyon cienegas, the seasonal cycle of wetting in the winter followed by drying in summer may provide such conditions. However, the second piezometer sample (PZ7) with a sulfate isotope signature indicating oxidation of sulfide is not located in an area with a clear source of pyrite-rich sediments or secondary pyrite oxidation processes. PZ7 is located in a typical, narrow, dry stretch of the wash with semi-arid vegetation and surface flows during storm runoff events.

The springs and groundwater samples with a higher $\delta^{34}S_{(SO4)}$ signature (>9.0‰) have two possible explanations (Figure 8). Samples SP1, WL13, and WL14 are at the mountain front in close proximity to limestone bedrock deposited in shallow water environments (Bittson 1976), which may indicate gypsum dispersed in limestone, or sulfate incorporated in other ways in limestone (e.g., fluid inclusions and/or structurally in calcite). The remaining spring and piezometer samples SP5, SP10, SP16, PZ4 and PZ8 in the LCNCA have higher $\delta^{34}S_{(SO4)}$ values (≥9.5‰) likely from bacterial sulfate reduction (BSR) (Clark and Fritz 1997). These samples have low dissolved oxygen values, which is consistent with anoxic conditions necessary for BSR. Groundwater from WL12 has a $\delta^{34}S_{(SO4)}$ value of +10.7‰ and 100% dissolved oxygen content, which may be explained by interaction with local sulfate-bearing sediments weathered from the Santa Rita Mountains.

Geochemical evolution of groundwater across the study area.

Previous studies found that groundwater evolves from a Ca-Mg-HCO_3 type water at the mountain front to a Na-HCO_3 type water in the LCNCA (Huth 1996). The thick basin-fill unit is dominated by fanglomerates and mudflow units along Gardner Canyon (Figure 13), likely providing large clay surface areas for cation-exchange processes. This study does not show as clear a geochemical evolution pattern as previous studies, which may be due to the lack of dense sampling at the mountain front. The highest Ca^{2+}/Na^{+} ratios were found at the mountain front with the exception of WL38 where the age tracers indicate older water, however the Ca^{2+}/Na^{+} ratio is within the range of the samples in the basin center, away from the mountain front (Figure 10). Two wells (WL15 and WL37), ~6450m apart, along Gardner Canyon, east of the mountain front, have almost identical Ca^{2+}/Na^{+} ratios, which do not fit the expected pattern of geochemical evolution of water as it moves downgradient. Most of the wells and spring samples including all the LCNCA groundwater samples have Ca^{2+}/Na^{+} mass ratios <6. The similar Ca^{2+}/Na^{+} ratios in the springs that feed the cienegas and underlying groundwater in the LCNCA provide further evidence that the cienegas are dependent on the basin-fill aquifer (Figure 9).

Revisions to the Conceptual Model in the Upper CCW for Basin Hydrogeology

This study refines how flow paths through the Santa Rita mountain block system and diffuse recharge mechanisms vary across the basin to Cienega Creek (Figure 15), from the effects of major fault zones on the study area's western boundary to the clay-rich units in the underlying basin-fill and Pantano Formation (Figure 13) and high ET due to widespread grasslands and riparian areas. The understanding of current conceptual models of the Cienega Creek watershed display infiltration of precipitation through the Santa Rita mountain block, mountain front, and diffuse recharge with similar contributions to the basin aquifer. The foothills of the Santa Rita Mountains, where mountain front recharge is considered the major component of recharge to the basin-fill aquifer (Osterkamp 1973; Huth 1996), has been identified as the source of groundwater surrounding Empire Ranch, west of Cienega Creek in the LCNCA (Harshbarger and Assoc. 1975).

In this study, groundwater was found to be predominately recharged prior to the 1950's based on low tritium values and adjusted radiocarbon ages up to 27,000 years old, which may be a result of deep, long flow paths through the mountain block or slow recharge through fractures orthogonal to the major fault zones. Groundwaters across the basin were recharged at the mountain front (1600 ±200m) and/or higher elevations from summer and winter precipitation based on the stable water isotope results. There was little to no evidence of diffuse basin recharge or focused ephemeral wash recharge to the basin aquifer system. Well logs and major ion chemistry indicate clay-confining units in the upper basin-fill likely limit vertical groundwater movement, like found in the San Pedro Basin (Hopkins et al. 2014). The lateral extent of the clay-confining units has not been identified in previous studies, however evidence by quasi-artesian wells found in the LCNCA allude to a shallow unconfined basin-fill aquifer and possible deeper regional aquifer (Harshbarger and Assoc. 1975).

CONCLUSIONS

Mid- to high elevation winter and summer precipitation is the main source of recharge to the Santa Rita Mountains and the adjacent basin-fill aquifer in the Cienega Creek watershed. The basin-fill aquifer is dominated by older water recharged prior to the 1950's and up to tens of thousands of years old, indicating modern recharge is minimally reaching the water table. Low sulfate concentrations and an atmospheric sulfur isotope signature indicate groundwater, for the most part, does not come in contact with sulfur bearing rocks as the water moves from the Santa Rita mountain front to Cienega Creek. A few groundwater samples show evidence of pyrite oxidation, gypsum dissolution, and bacterial sulfate reduction. The springs located in the LCNCA that feed the cienegas are sustained by the shallow basin-fill aquifer, recharged at the mountain front and/or higher elevations (mountain block) and not by recent local precipitation (e.g., monsoon floodwaters). The combination of relatively old groundwater and limited modern recharge across the study area indicates that groundwater resources and the hydrologically connected riparian areas and associated aquatic life are vulnerable to over-extraction from unregulated groundwater use.

Possible Future Study Questions:

- Why are there cienegas in the LCNCA and what controls their spatial location?
- What conservation practices should be implemented to minimize impacts to groundwater resources in the basin?
- How do the different tributaries influence the water chemistry of Cienega Creek as it evolves from the headwaters downstream to the outlet?
- Is there a deeper confined regional aquifer or localized smaller confined aquifers in the LCNCA?
- What geochemical or biological processes control the black waters of Oak Tree Canyon and is nearby Road Well hydrologically connected to the cienegas in Oak Tree canyon?
- What contributions (if any) are there of mountain front recharge to the shallow basin-fill aquifer and focused recharge along ephemeral washes surrounding the western border of the study area?

FIGURES

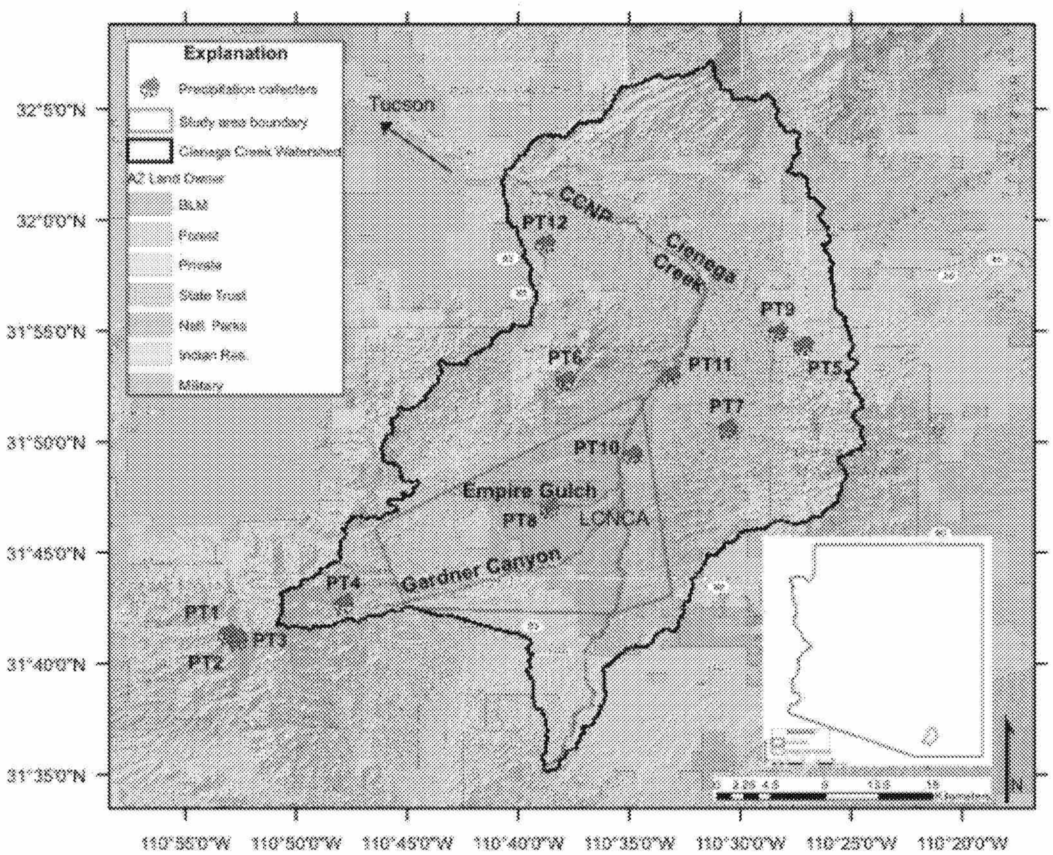

Figure 1: Land ownership map with precipitation (PT) collector locations. The inset map is the state of Arizona with the CCW boundary in blue.

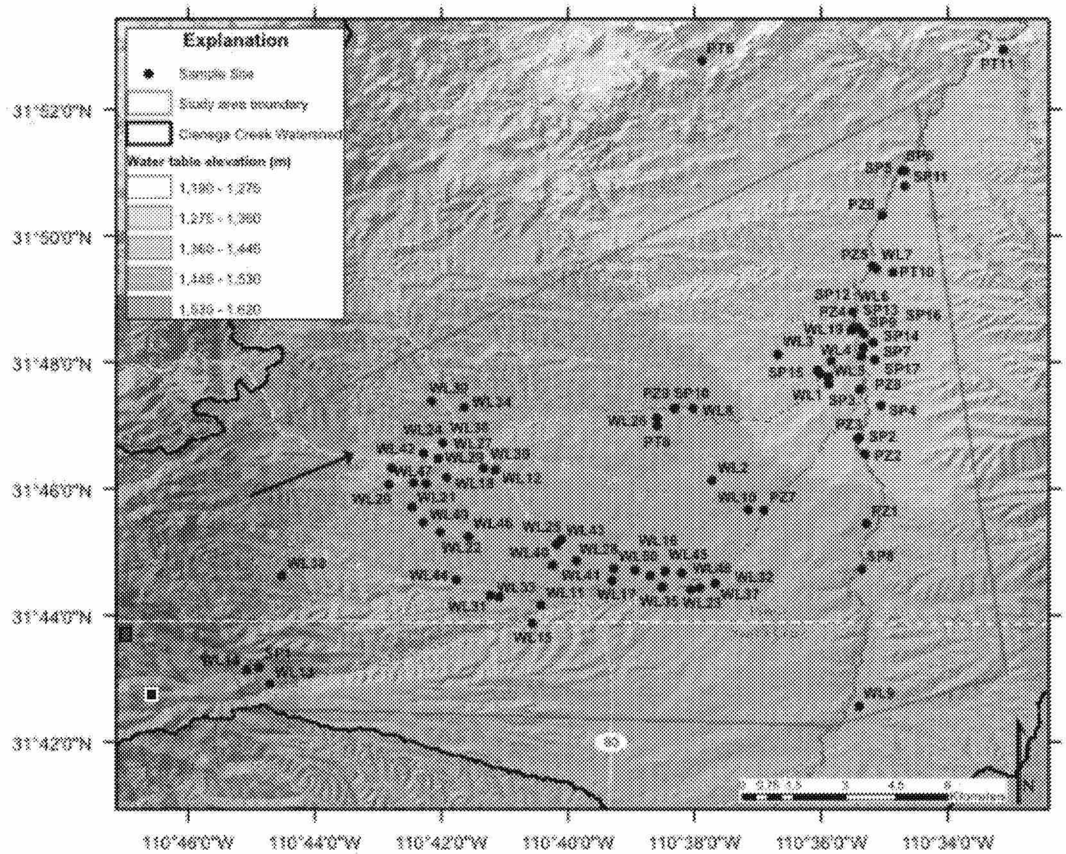

Figure 2: Sample site map. Locations of piezometers (PZ), precipitation (PT), springs (SP), and well (WL) samples collected as part of this study. Black arrow indicates groundwater flow direction. The red square symbol is the location for Cave of the Bells and the black square symbol is Onyx Cave.

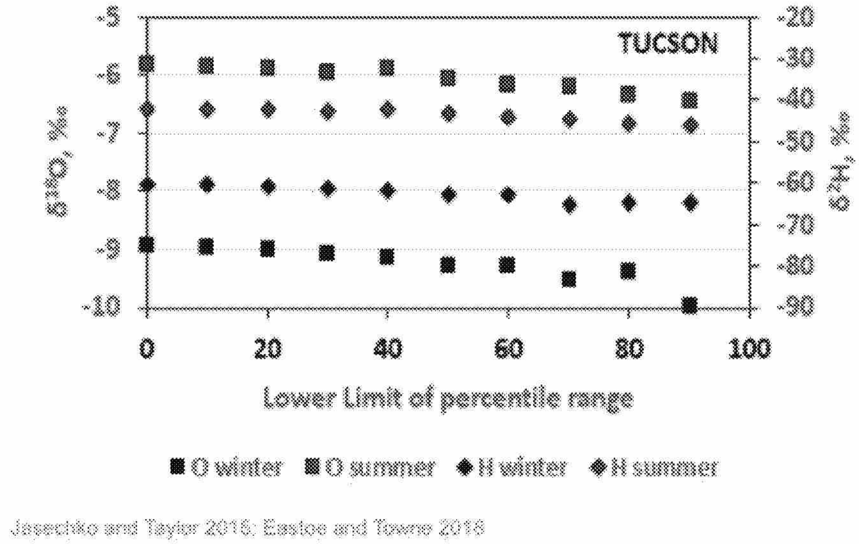

Figure 3: Plot of stable water isotopes for summer (June-October) and winter (November-May) rainfall intensity effect, Tucson, Arizona (740m above sea level). Weighted means for each isotope for each month were calculated using the long term (30-year record) precipitation data (Eastoe and Dettman 2016; Eastoe and Towne 2018, unpublished data for 2013 to 2015). Months with precipitation were ranked from 0^{th} (driest) to 100^{th} (wettest) percentile according to precipitation total. The set of points plotted at the 70 point on the x-axis (lower limit of percentile range) corresponds to the amount-weighted means of $\delta^{18}O$ and $\delta^{2}H$ for the 70^{th} to 100^{th} percentile of months (i.e. the wettest 30% of months), and so on.

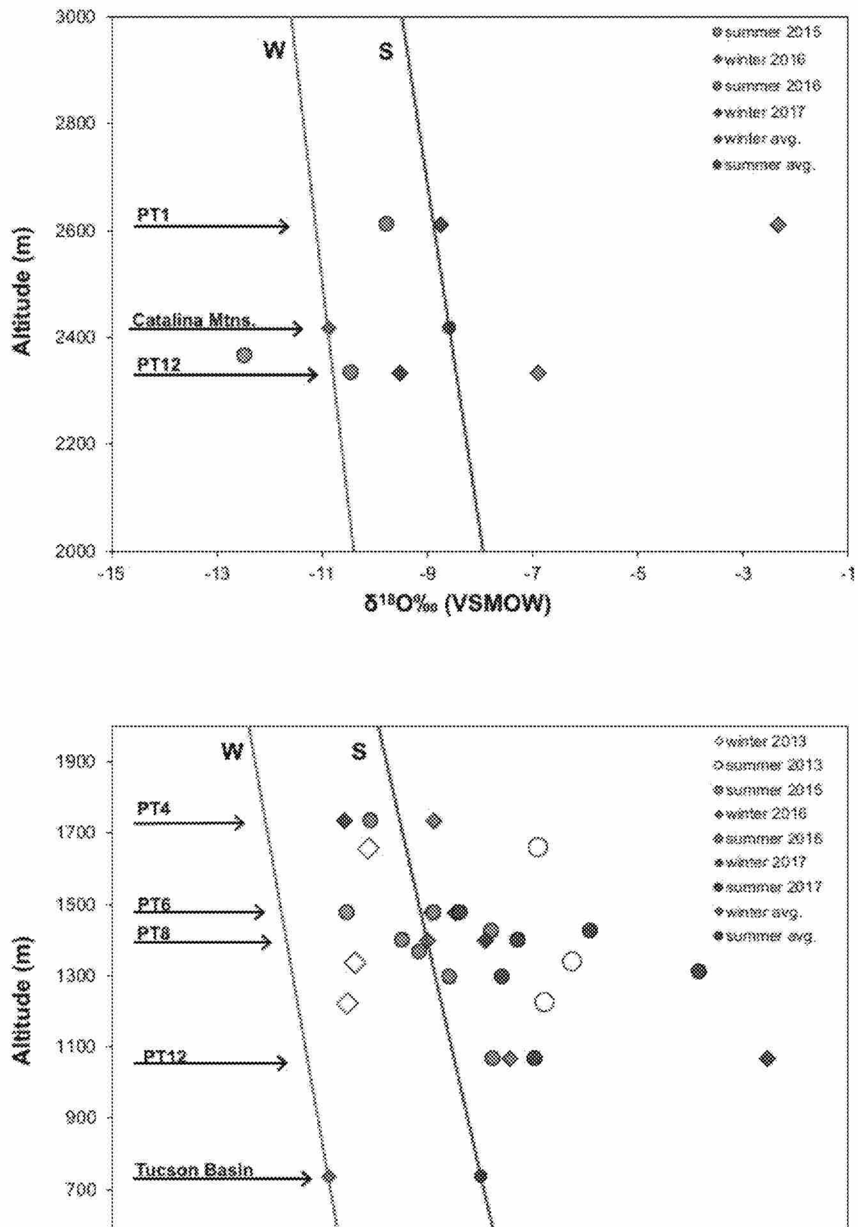

Figure 4: (A) Plot of altitude vs. $\delta^{18}O$ of seasonal precipitation (PT) samples collected at high altitude. (B) Plot of altitude vs. $\delta^{18}O$ of seasonal precipitation (PT) samples. Precipitation samples for the year 2013 are from Hudbay Minerals Inc. and are arithmetic averages of several collections during each season. Other data are for single collections representing entire seasons. Winter (W) and summer (S) trendlines were created from data as long term amount-weighted means for each season collected at the University of Arizona in Tucson Basin and Palisades Ranger Station in the Santa Catalina Mountains (Eastoe and Dettman 2016; Wright 2001).

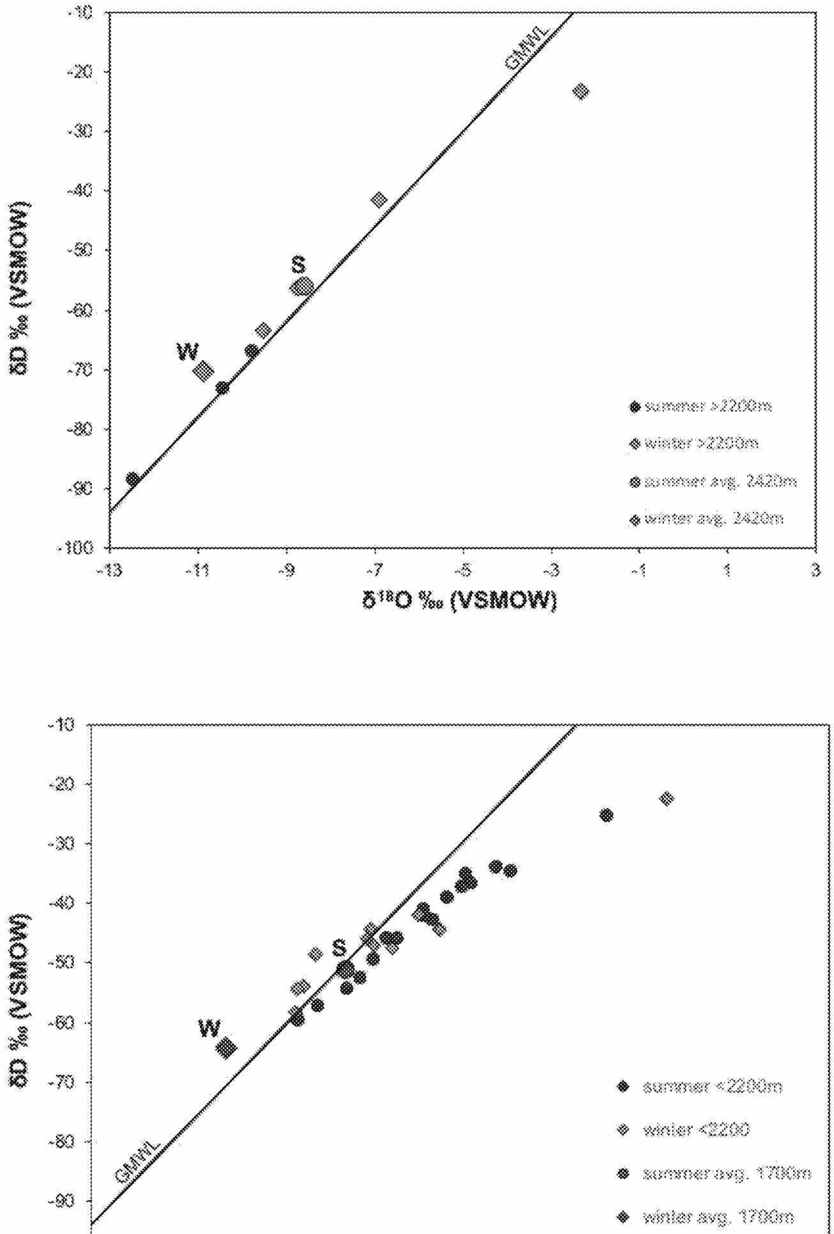

Figure 5: (A) Plot of δD vs. $\delta^{18}O$ for high altitude seasonal precipitation samples collected in the CCW. Solid green symbols indicate long term amount-weighted winter and summer means of precipitation collected at the Palisades Ranger Station in the Santa Catalina Mountains, Arizona (Wright 2001). (B) Plot of δD vs. $\delta^{18}O$ for low altitude seasonal precipitation samples collected in the CCW. Solid purple symbols indicate long term amount-weighted winter and summer means of precipitation collected at the University of Arizona in Tucson Basin, Arizona (Eastoe and Dettman 2016). The global meteoric water line (GMWL) is from Craig (1961).

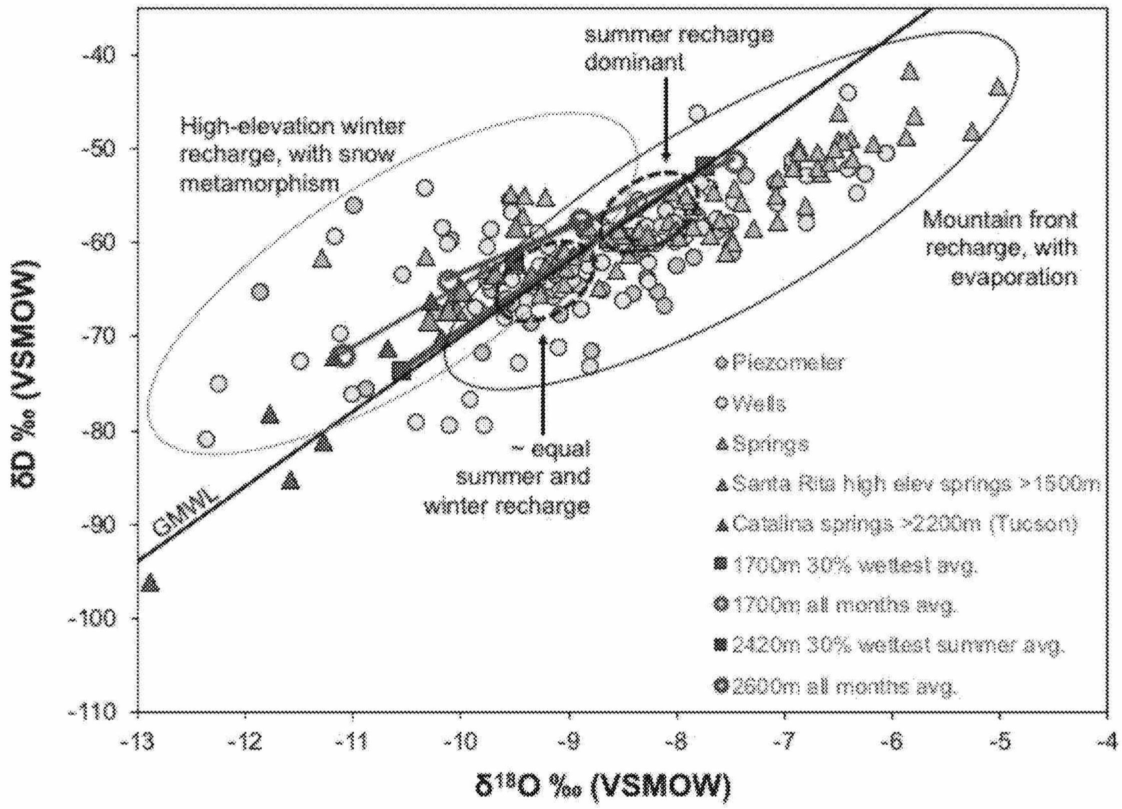

Figure 6: Plot of δD vs. $\delta^{18}O$ for all groundwater samples collected as part of this study. The global meteoric water line (GMWL) is from Craig (1961). Also shown are local meteoric water lines (LMWLs) for 1700m and 2600m elevation (see text for explanation).

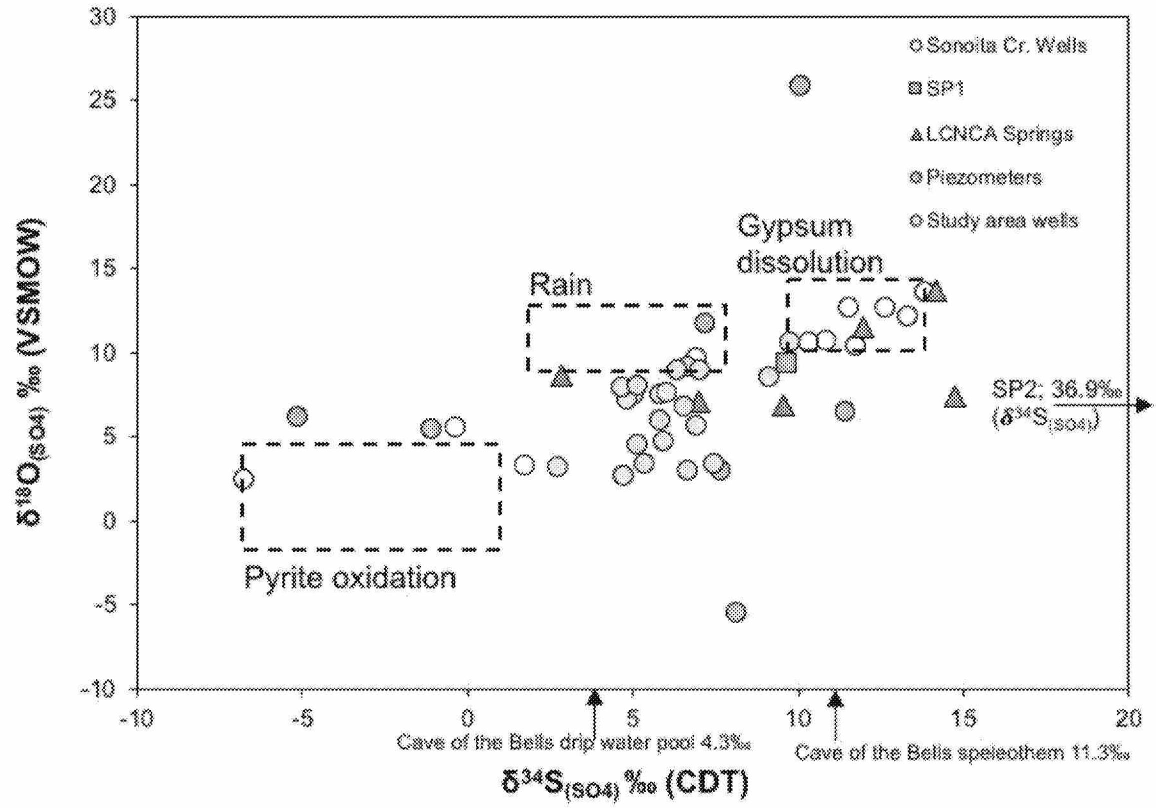

Figure 7: Plot of $\delta^{18}O_{(SO4)}$ vs. $\delta^{34}S_{(SO4)}$ with all available groundwater samples. SP2 has a $\delta^{18}O_{(SO4)}$ value of 7.0‰. Sonoita Creek wells and the black dotted boxes labeled pyrite oxidation, atmosphere, and gypsum dissolution are from Gu et al. (2008).

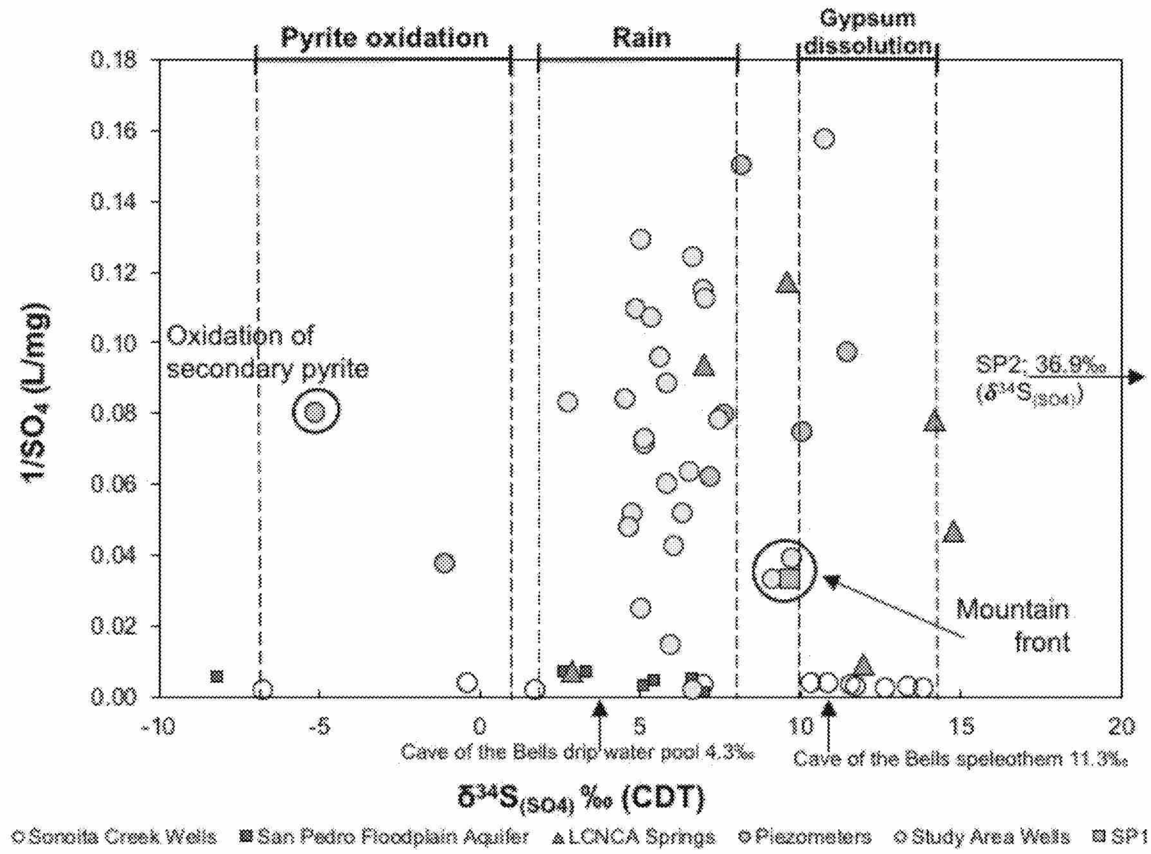

Figure 8: Plot of $1/SO_4$ vs. $\delta^{34}S_{(SO4)}$ with all available groundwater samples. SP2 has a $1/SO_4$ value of 0.09 (L/mg). Sonoita Creek wells (Gu 2005), and San Pedro floodplain aquifer sulfate concentrations (Hopkins et al. 2014) are shown to emphasize the contrast between high sulfate concentrations in those studies and low sulfate concentrations from this study.

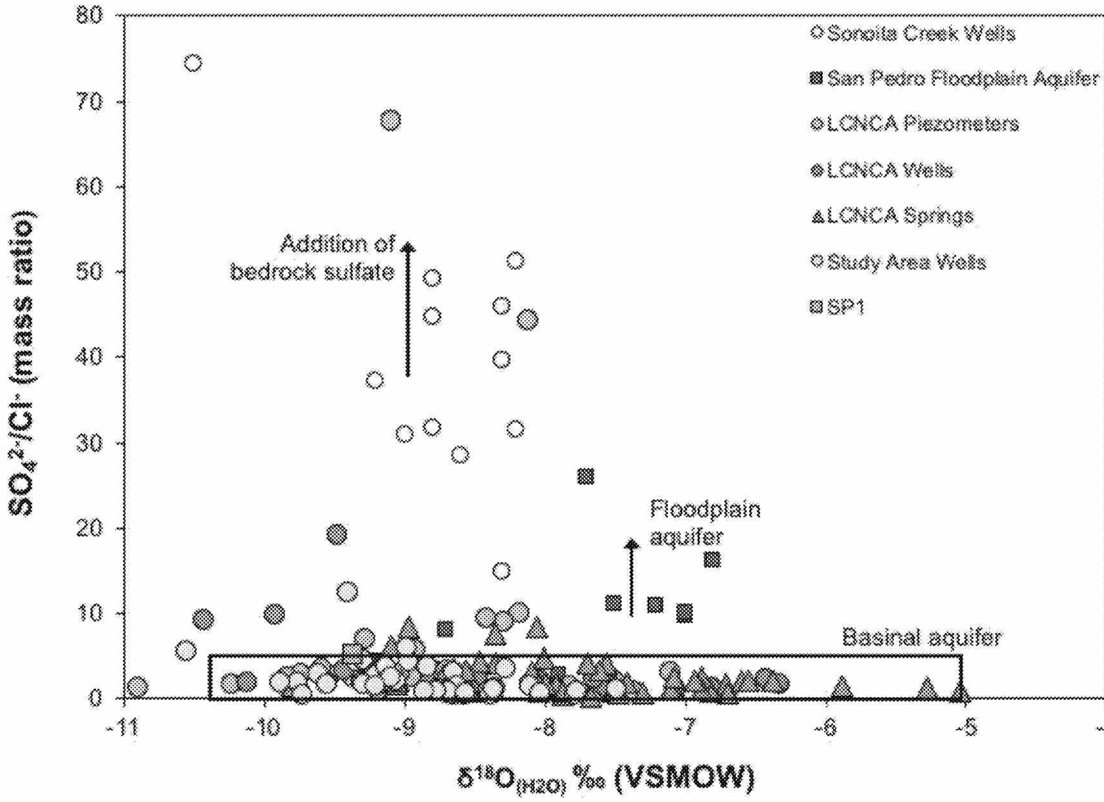

Figure 9: Plot of SO_4^{2-}/Cl^- ratios vs. $\delta^{18}O_{(H2O)}$ for all available groundwater samples. Sonoita Creek wells (Gu et al. 2008), and San Pedro floodplain aquifer (Hopkins et al. 2014) display increased sulfate concentrations from sulfur bearing rocks. The black solid outline box shows the basin-fill aquifer samples for this study area.

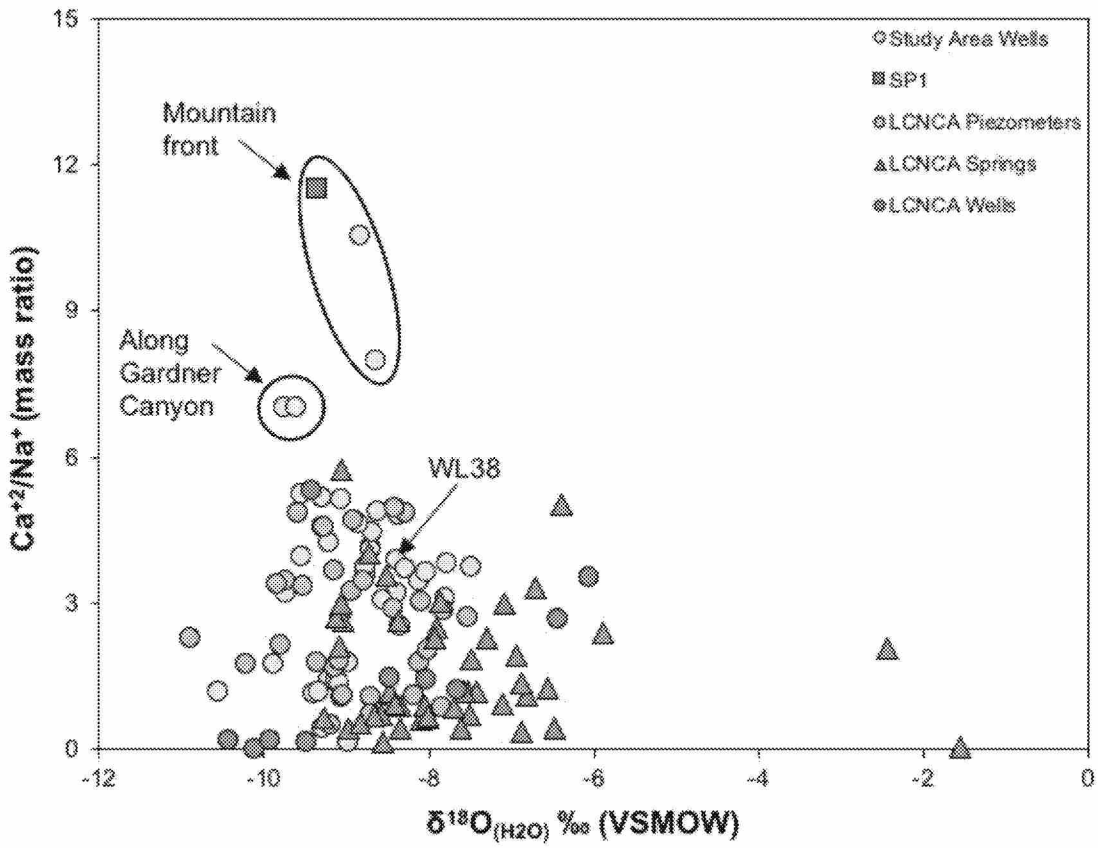

Figure 10: Plot of Ca^{+2}/Na^{+} vs. $\delta^{18}O_{(H2O)}$ for all groundwater samples collected as part of this study.

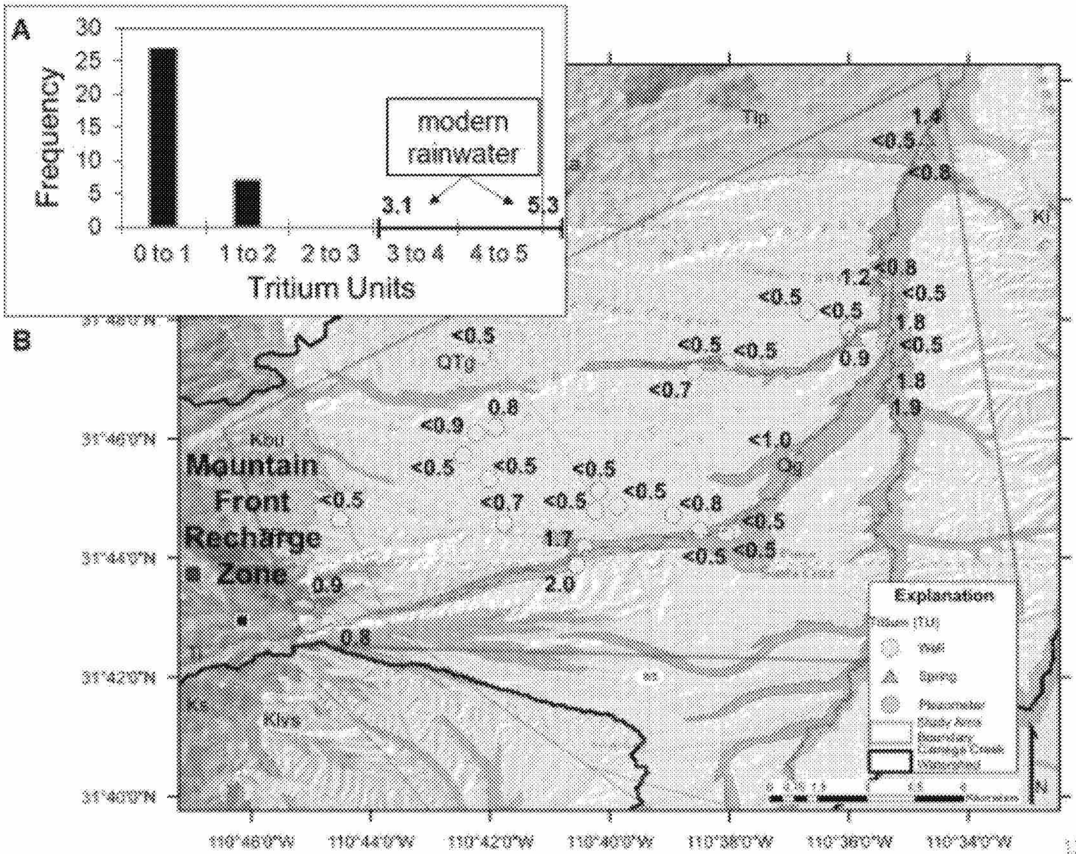

Figure 11: (A) Histogram of groundwater sample frequency for tritium values. (B) Tritium distribution map of all groundwater samples collected for this study. The red square symbol is the location for Cave of the Bells and the black square symbol is Onyx Cave.

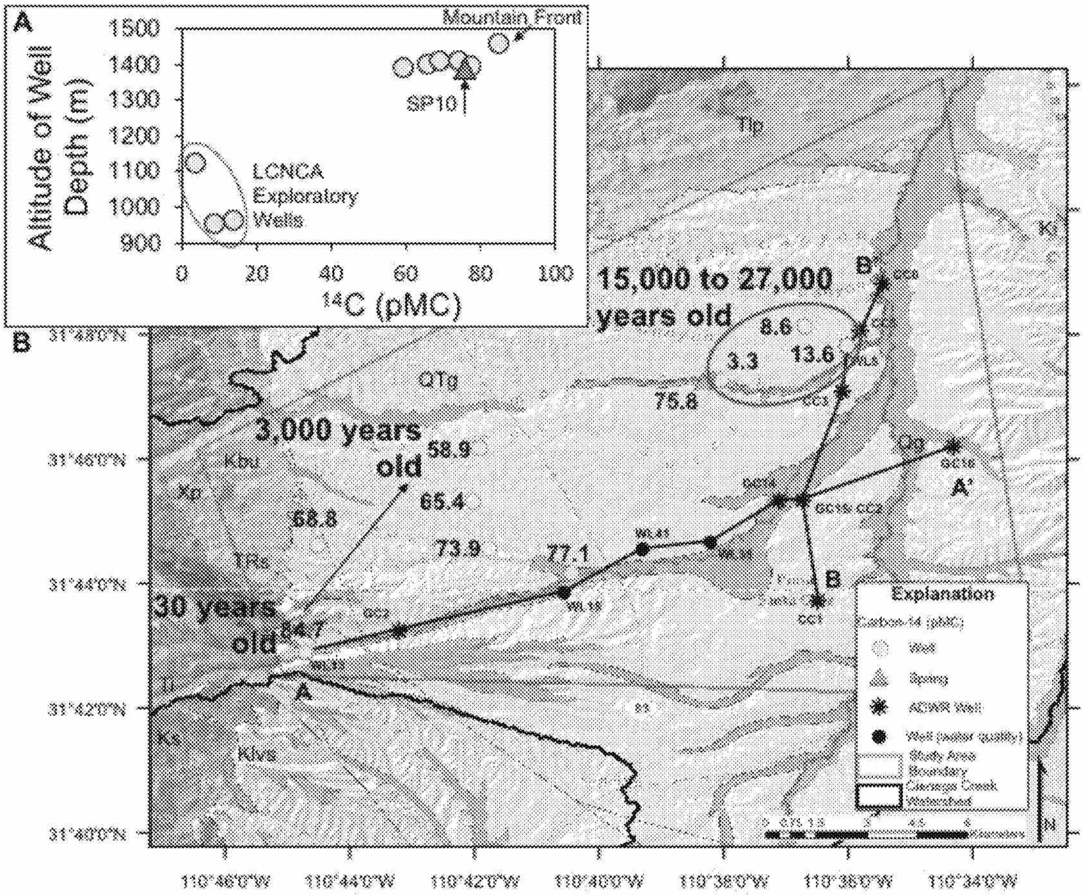

Figure 12: (A) Plot of well depth altitudes vs. ^{14}C for all available groundwater samples. (B) ^{14}C distribution map of all groundwater samples available. Adjusted ages, representing travel times from the mountain front down gradient, are reported. Cross sections (A to A' and B to B') can be seen in Figures 12 and 13.

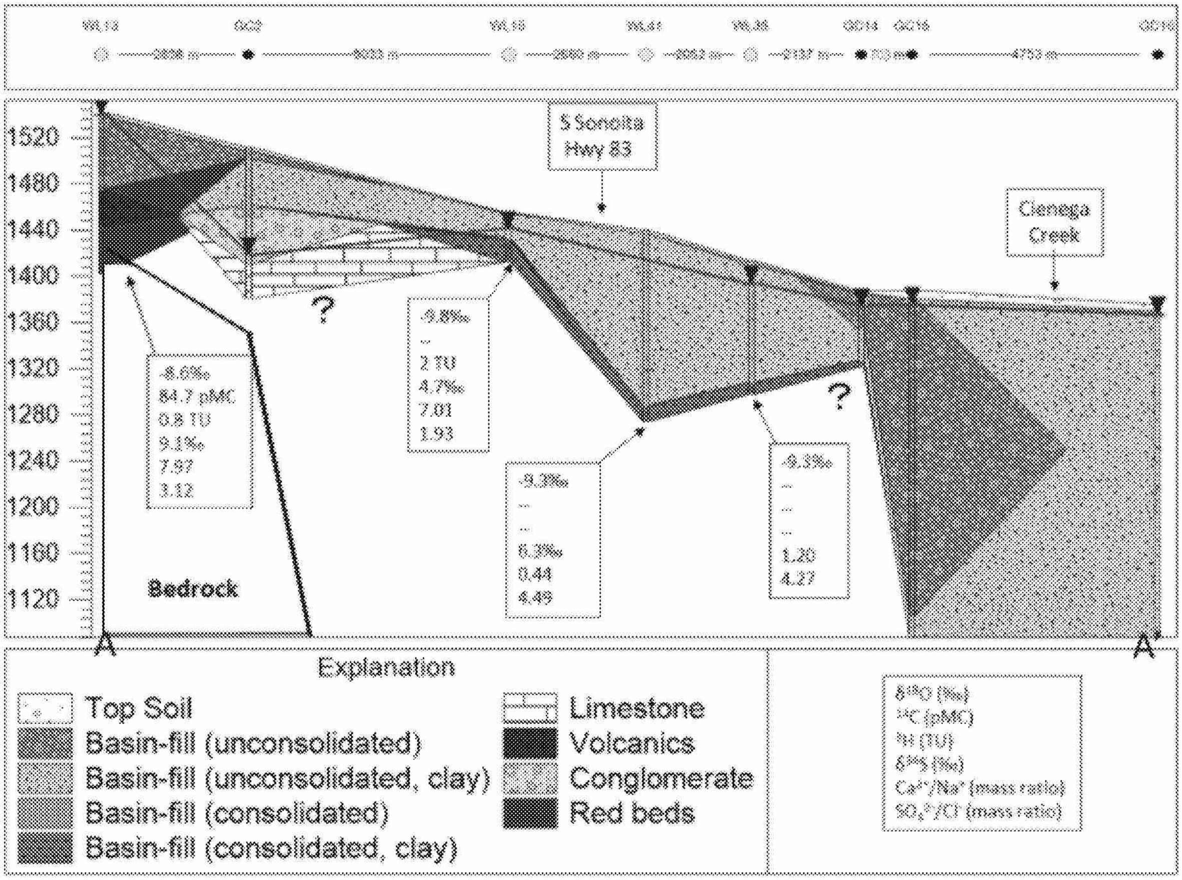

Figure 13: Lithologic cross section from Figure 10, west (A) to east (A'), constructed from driller's logs. The blue triangles are static water levels in the wells reported by Arizona Department of Water Resources (ADWR).

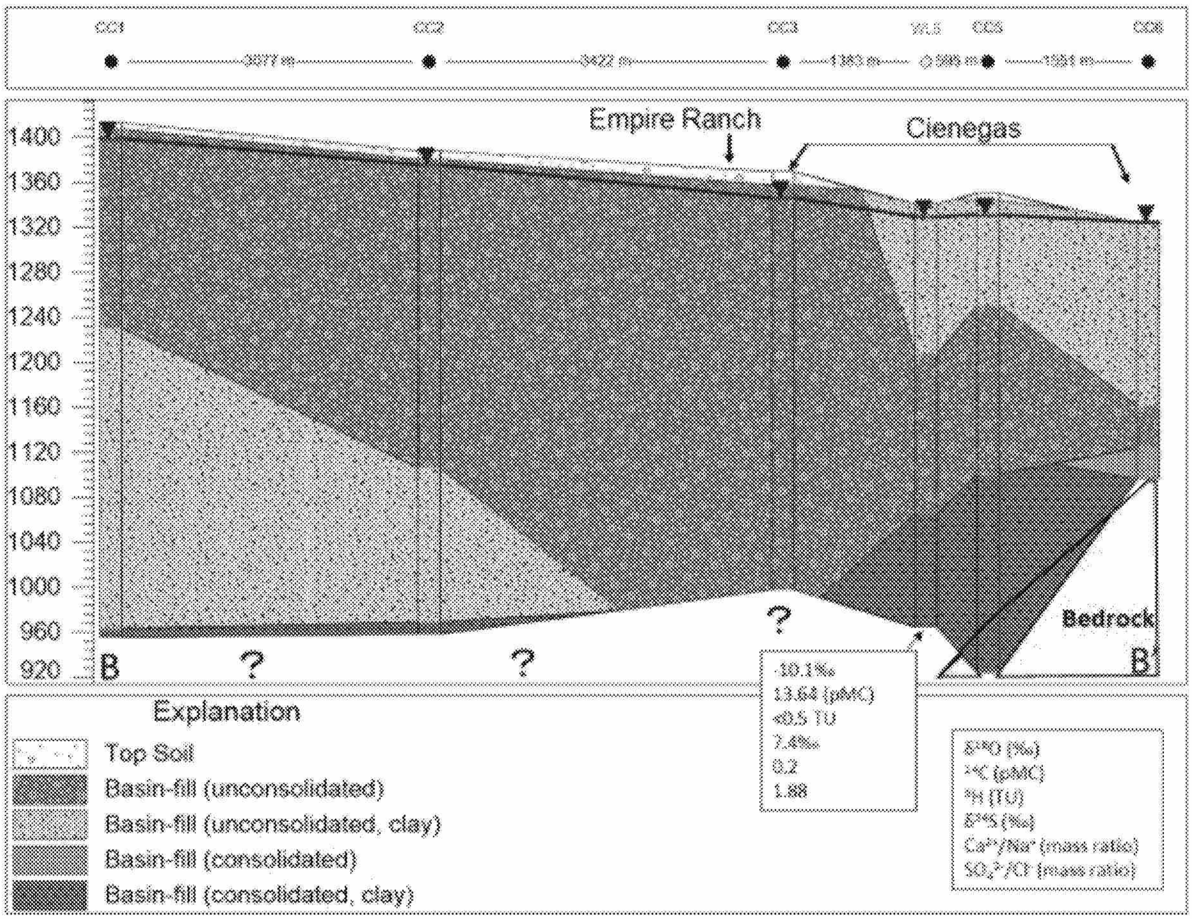

Figure 14: Lithologic cross section from Figure 10, south (B) to north (B'), constructed from driller's logs. The blue triangles are static water levels in the wells reported by Arizona Department of Water Resources (ADWR).

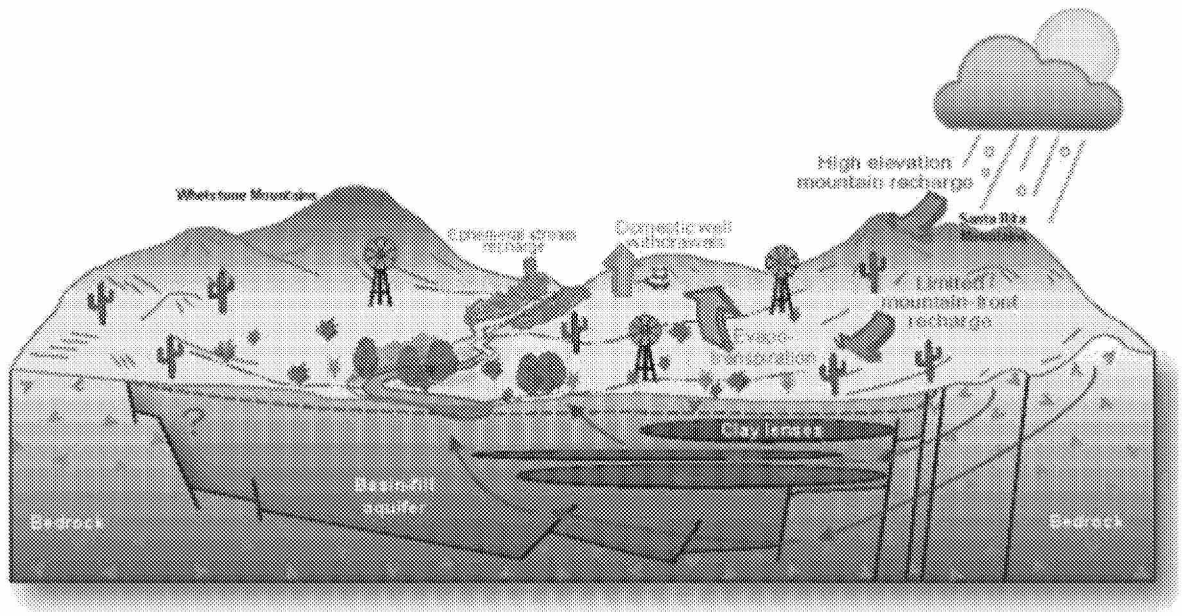

Tillman 2011 (modified)

Figure 15: Revised conceptual model for Upper Cienega Creek Watershed study area.

TABLES

Table 1: Sample locations

Sample ID	Sample Type	Latitude (Decimal Degrees)	Longitude (Decimal Degrees)	Altitude (m)	Well Depth (m)	Depth to Water (m)	Screened Interval (m)
PT1	Precipitation	31.68881	-110.88503	2616			
PT2	Precipitation	31.68611	-110.87847	2368			
PT3	Precipitation	31.68369	-110.87728	2336			
PT4	Precipitation	31.71105	-110.79800	1740			
PT5	Precipitation	31.90544	-110.45292	1538			
PT6	Precipitation	31.87956	-110.63139	1482			
PT7	Precipitation	31.84282	-110.50986	1430			
PT8	Precipitation	31.78353	-110.64322	1402			
PT9	Precipitation	31.91604	-110.47183	1370			
PT10	Precipitation	31.82384	-110.58112	1314			
PT11	Precipitation	31.88266	-110.5521	1301			
PT12	Precipitation	31.98167	-110.64664	1070			
PZ1	Piezometer	31.75773	-110.58807	1372			
PZ2	Piezometer	31.77591	-110.58855	1339			
PZ3	Piezometer	31.78031	-110.59009	1338			
PZ4	Piezometer	31.80927	-110.59029	1320			
PZ5	Piezometer	31.82550	-110.58657	1317			
PZ6	Piezometer	31.83904	-110.58405	1308			
PZ7	Piezometer	31.76112	-110.61505	1377			
PZ8	Piezometer	31.79315	-110.58978	1337			
PZ9	Piezometer	31.78800	-110.63841	1393			
SP1	Spring	31.71993	-110.74790	1578			
SP2	Spring	31.78013	-110.59042	1345			
SP3	Spring	31.79437	-110.59800	1344			
SP4	Spring	31.78860	-110.58431	1344			
SP5	Spring	31.85065	-110.57801	1293			
SP6	Spring	31.85047	-110.57865	1303			
SP7	Spring	31.80187	-110.58952	1324			
SP8	Spring	31.74567	-110.58943	1328			
SP9	Spring	31.80760	-110.58880	1328			
SP10	Spring	31.78777	-110.63863	1389			
SP11	Spring	31.84650	-110.57799	1301			
SP12	Spring	31.80863	-110.59217	1315			
SP13	Spring	31.80933	-110.59160	1315			
SP14	Spring	31.80885	-110.59124	1315			

Sample ID	Sample Type	Latitude (Decimal Degrees)	Longitude (Decimal Degrees)	Altitude (m)	Well Depth (m)	Depth to Water (m)	Screened Interval (m)
SP15	Spring	31.79633	-110.59810	1331			
SP16	Spring	31.80534	-110.58631	1326			
SP17	Spring	31.80075	-110.58596	1341			
WL1	Well	31.79818	-110.60091	1341			
WL2	Well	31.76907	-110.62866	1403			
WL3	Well	31.80219	-110.61144	1349	392		
WL4	Well	31.80066	-110.59730	1351			
WL5	Well	31.79716	-110.60021	1341	377		
WL6	Well	31.81335	-110.59166	1329			
WL7	Well	31.82484	-110.58544	1318			
WL8	Well	31.78799	-110.63369	1384	258		
WL9	Well	31.70948	-110.59011	1414			
WL10	Well	31.76145	-110.61918	1384			
WL11	Well	31.73630	-110.67377	1442	44		
WL12	Well	31.77176	-110.68566	1508	83	70	61-88
WL13	Well	31.71535	-110.74512	1550	88	2	58-76
WL14	Well	31.71905	-110.75121	1588	122		
WL15	Well	31.73135	-110.67606	1447	73	10	24-44
WL16	Well	31.74539	-110.64907	1427	178	23	
WL17	Well	31.74414	-110.64500	1428	160	26	142-160
WL18	Well	31.76826	-110.70389	1528	140	85	116-140
WL19	Well	31.80396	-110.58897	1330			
WL20	Well	31.76204	-110.70757	1520	110	85	98-110
WL21	Well	31.76841	-110.70731	1531	122	99	122-140
WL22	Well	31.75544	-110.70036	1514	110	76	91-110
WL23	Well	31.74100	-110.64181	1424	122	12	104-122
WL24	Well	31.77887	-110.69962	1490	123	60	
WL25	Well	31.75353	-110.66840	1468			
WL26	Well	31.78544	-110.64319	1404			
WL27	Well	31.77491	-110.70078	1516	98	79	
WL28	Well	31.74777	-110.66452	1455	180	32	
WL29	Well	31.76969	-110.69858	1519	122	91	98-110
WL30	Well	31.77227	-110.68874	1508	152		122-152
WL31	Well	31.73826	-110.68476	1459	61	34	
WL32	Well	31.74067	-110.63196	1405	85	12	73-85
WL33	Well	31.73861	-110.68712	1457	61	35	0.3-61
WL34	Well	31.78813	-110.69392	1498	91	62	

Sample ID	Sample Type	Latitude (Decimal Degrees)	Longitude (Decimal Degrees)	Altitude (m)	Well Depth (m)	Depth to Water (m)	Screened Interval (m)
WL35	Well	31.74479	-110.63671	1413	116	19	104-116
WL36	Well	31.77619	-110.70454	1497	107	66	76-91
WL37	Well	31.74184	-110.62786	1398	71	12	30-37, 40-71
WL38	Well	31.74400	-110.74186	1559	143	110	119-143
WL39	Well	31.78983	-110.70251	1519	127	88	114-127
WL40	Well	31.74660	-110.67072	1465	137	30	
WL41	Well	31.74267	-110.65502	1433	166	152	148-166
WL42	Well	31.77238	-110.71299	1537	116	106	
WL43	Well	31.75218	-110.66962	1459	59	44	47-59
WL44	Well	31.74281	-110.69601	1479	65	41	
WL45	Well	31.74519	-110.64110	1416			
WL46	Well	31.75432	-110.69286	1494	91	68	79-91
WL47	Well	31.76796	-110.71380	1546	156	115	
WL48	Well	31.74020	-110.63434	1404	104	11	85-98
WL49	Well	31.75794	-110.70480	1515	110	79	91-110
WL50	Well	31.74589	-110.65458	1442	189	21	110-140, 171-189

Table 2: Field Parameters

Sample ID	Date	Dissolved Oxygen (%)	Specific Conductance (µs/cm)	pH	Temp (°C)
PZ2	03/12/16	33.8		7.41	17.6
PZ2	05/21/16	27.1		7.16	24.1
PZ2	08/28/16	58.6	339.1	7.81	22.4
PZ2	12/18/16	48.4	353.5	7.74	16.8
PZ3	03/12/16	9.1		6.99	14.7
PZ3	08/28/16	20.5	376.4	7.80	21.8
PZ3	12/18/16	18.7	382.2	7.70	14.7
PZ4	01/31/16	19.3		7.64	13.3
PZ4	05/14/16	7.4		7.39	18.8
PZ4	08/27/16	4.1	377.3	8.06	21.4
PZ4	12/17/16	40.4	381.5	7.98	13.8
PZ5	03/13/16	50		8.27	22.0
PZ5	05/21/16	18.2		7.89	19.1
PZ5	08/27/16	31.4	420.1	7.41	25.6
PZ5	11/26/16			8.11	17.7
PZ6	05/22/16	46.3		8.04	23.5
PZ6	08/27/16				
PZ6	11/26/16		1364.3	8.14	20.8
PZ7	01/31/16	13.5	430	7.03	17.1
PZ7	05/14/16	8.4		7.17	19.4
PZ7	08/28/16	29	462	7.40	22.8
PZ7	11/25/16		479.3	7.63	18.7
PZ8	03/12/16	4.5		7.07	16.3
PZ8	05/21/16				
PZ8	08/28/16	97.8	449.5	7.52	21.1
PZ8	12/18/16	41.7	633.2	7.37	17.0
PZ9	01/31/16	5.1		7.12	18.1
PZ9	05/14/16	19.2		6.83	17.8
PZ9	08/28/16	27.4	545	7.28	19.6
PZ9	11/25/16		533.4	7.76	17.3
SP1	05/19/16	63.9	569	7.30	22.3
SP2	03/12/16	20.4		7.29	15.3
SP2	05/21/16	16.9		7.16	17.2
SP2	08/28/16				
SP2	08/28/16	11.5	373	7.57	19.6
SP2	12/18/16	16.2	1655.1	7.25	8.7
SP3	05/22/16	11.5		6.89	16.3

Sample ID	Date	Dissolved Oxygen (%)	Specific Conductance (µs/cm)	pH	Temp (°C)
SP3	08/27/16	0.3	615	7.26	30.2
SP3	12/17/16	25.8	830.7	7.66	9.5
SP4	02/28/16	110		8.88	22.5
SP4	09/25/16		712	7.20	18.7
SP4	12/18/16	8.9	391.7	7.36	15.8
SP5	03/13/16	11.3		6.83	13.4
SP5	06/05/16				
SP5	09/02/16		497	7.29	20.1
SP5	11/26/16		834	7.71	11.7
SP6	03/13/16	21		6.72	19.6
SP6	06/05/16	16.2		7.17	17.9
SP6	09/02/16		638.6	7.34	21.8
SP6	11/26/16		485.1	7.47	14.4
SP7	01/31/16	75.3		7.71	15.4
SP7	05/14/16	3.3		6.89	20.0
SP7	08/27/16	2.3	804.5	7.15	22.8
SP7	12/17/16	68.8	625.2	7.71	9.0
SP8	02/27/16	28		7.50	17.0
SP8	05/14/16	3.4		6.81	19.2
SP8	08/27/16	0.2	649	7.16	23.2
SP8	12/17/16	0.5	353.8	7.50	14.5
SP9	02/27/16	64		8.13	16.2
SP10	01/31/16	6.1		7.20	13.0
SP10	05/19/16	101.9	830	7.11	19.5
SP10	08/28/16	6.4	826	7.05	20.0
SP10	11/25/16		664.7	7.80	16.3
SP11	03/13/16	59.4		7.43	16.3
SP11	06/05/16	65.4	379	7.11	14.7
SP11	09/02/16		855.9	7.24	23.0
SP11	11/26/16		703.8	7.71	13.4
SP12	02/27/16	7.2		7.10	14.8
SP12	05/14/16	40		7.46	30.5
SP12	12/17/16	3.4	1234.2	7.35	9.2
SP14	12/17/16	74.2	2396.6	8.08	7.2
SP15	03/12/16	95.7		7.62	13.4
SP15	12/18/16	18.6	3129.9	7.30	8.5
SP16	02/28/16	19.8		7.10	11.2
SP16	05/22/16	24		7.01	14.5

Sample ID	Date	Dissolved Oxygen (%)	Specific Conductance (µs/cm)	pH	Temp (°C)
SP16	09/02/16		492	7.40	18.1
SP16	12/16/16	8.9	506.5	7.74	9.2
SP17	09/25/16		521.7	7.03	19.0
SP17	12/16/16	38.8	393.6	8.02	17.8
WL3	08/03/16	0.8	1027	9.36	22.5
WL5	08/03/16	63.9	309	9.42	24.9
WL7	02/27/16	48.7		7.05	18.6
WL7	05/21/16	49.2		6.98	18.2
WL7	08/27/16	75.9	400	8.06	19.0
WL7	12/16/16	48.8	397.8	7.88	17.4
WL8	08/03/16	36.2	348	7.65	24.3
WL8	08/27/16	40.7	341	8.07	25.5
WL11	08/03/16	81.1	270.6	7.70	19.6
WL12	05/29/16	99.6	377	7.45	21.8
WL13	06/01/16	72.4	543	7.13	19.2
WL14	05/19/16	71	544	7.44	22.0
WL15	04/09/16	82.6		7.14	18.5
WL16	05/30/16	100.6	219.4	7.99	22.9
WL17	05/30/16	91.3	203	7.78	22.7
WL18	04/05/14	81.2	365	7.40	19.9
WL20	04/05/14	80.6	356	7.26	21.5
WL21	04/09/16	91.7		7.27	22.1
WL22	05/29/16	96.6	335	7.55	21.8
WL23	05/30/16	90.4	254.8	7.87	23.3
WL24	04/09/16	60		7.85	16.8
WL25	05/30/16	103.6	314	7.77	24.1
WL26	04/05/14	81.9	472	7.76	18.6
WL27	05/28/16	104.1	369	7.43	22.7
WL28	04/09/16	90.3	382	6.94	21.5
WL29	05/28/16	100.7	346	7.50	22.6
WL30	05/29/16	98	383	7.38	22.1
WL31	05/20/16	95.8	296	7.49	22.0
WL32	05/20/16	84.8	278.7	7.69	23.1
WL33	05/20/16	104.1	339	7.75	20.1
WL34	05/28/16	98.3	357	7.55	22.9
WL35	05/28/16	97.2	249.9	7.75	25.2
WL36	06/01/16	93.9	363	7.34	22.0
WL37	04/09/16	101.1	360	6.90	21.6

Sample ID	Date	Dissolved Oxygen (%)	Specific Conductance (µs/cm)	pH	Temp (°C)
WL38	05/14/16	86.7	681	6.70	22.0
WL39	04/09/16	72.5		7.65	16.7
WL40	05/29/16	85.2	364	7.70	21.8
WL41	05/29/16	69.5	292.2	7.80	24.4
WL42	03/26/16	58.5		7.45	22.0
WL43	05/20/16	98.3	345	7.33	21.1
WL44	04/09/16	90.8		7.34	19.9
WL44	05/14/16	96.9	365	7.46	21.5
WL45	05/28/16	96.5	208.3	7.96	24.7
WL46	05/30/16	91.8	331	7.31	21.0
WL47	03/26/16	63.9		7.39	21.8
WL48	05/20/16	93.1	256.1	7.50	23.0
WL49	05/30/16	97.2	353	7.55	22.5
WL50	05/14/16	47.2	334	7.70	23.5

Table 3: Methods

Analysis Type	Method	Precision	Detection Limit	Lab	Notes
Alkalinity	Gran-Alk Titration	NA	NA	HAS[1] Laboratory	Gieskes and Rogers (1973)
Anions	Dionex Ion Chromatograph (IC) model ICS-3000.	±2%	Dependent on initial standard concentrations and analyte being measured	HAS Laboratory	Dionex ion chromatography; AS23 analytical column
Cations	Perkins Elmer, Optima 5300DV, ICP-OES	±3%	Dependent on initial standard concentrations and analyte being measured	HAS Laboratory	Inductively-Coupled Plasma Optical Emission Spectrometer
$\delta^{18}O$	Los Gatos Research Isotope Analyzer model LWIA-24d	<0.08‰	NA	ASU[2] Isotope Lab	4th generation cavity enhanced absorption
δD	Los Gatos Research Isotope Analyzer model LWIA-24d	<0.9‰	NA	ASU Isotope Lab	4th generation cavity enhanced absorption
$\delta^{34}S_{(SO4)}$	ThermoQuest Finnigan Delta Plus XL	± <0.15‰	NA	EIL[3] UA Geosciences	continuous-flow gas-ratio mass spectrometer
$\delta^{18}O_{(SO4)}$	Thermo Electron Delta V	± <0.3‰	NA	EIL UA Geosciences	continuous-flow gas-ratio mass spectrometer
$\delta^{13}C$ DIC	Conventional Stable Isotope Mass Spectrometer	± -0.25‰	NA	AMS[4] Laboratory	continuous-flow gas-ratio mass spectrometer
$\delta^{13}C$ DIC	ThermoQuest Finnigan Delta Plus XL, coupled with a Gasbench automated sampler	± <0.30‰	NA	EIL UA Geosciences	continuous-flow gas-ratio mass spectrometer
^{14}C	NEC Pelletron AMS machine	±0.5%	0.2	AMS Laboratory	Tandum Accelerator built by National Electrostatics Corporation
^{3}H	Quantulus 1220 Spectrometer	NA	0.6 TU	EIL UA Geosciences	Liquid Scintillation Spectrometry

[1] HAS Hydrology and Atmospheric Sciences
[2] ASU Arizona State University
[3] EIL Environmental Isotope Laboratory
[4] AMS Accelerator Mass Spectrometry

Table 4: Isotopes

Sample ID	Date	$\delta^{18}O$ (‰)	δD (‰)	$\delta^{34}S_{(SO4)}$ (‰)	$\delta^{18}O_{(SO4)}$ (‰)	$\delta^{13}C$-DIC (‰) AMS	$\delta^{13}C$-DIC (‰) GEOS	Tritium (TU)	^{14}C-DIC (pMC)	Unadjusted age (years)	Adjusted age (years)
PT1	6/1/2016	-2.4	-23								
PT1	11/19/2016	-9.8	-67								
PT1	6/24/2017	-8.8	-56								
PT2	11/7/2015	-12.5	-88								
PT3	6/1/2016	-6.9	-41								
PT3	11/19/2016	-10.5	-73								
PT3	6/24/2017	-9.6	-63								
PT4	6/1/2016	-6.9	-47								
PT4	11/19/2016	-8.1	-57								
PT4	6/25/2017	-8.6	-58					4.1			
PT5	11/7/2015	-8.6	-59								
PT5	6/1/2016	-7.0	-44								
PT5	11/19/2016	-6.9	-49								
PT6	10/24/2016	-5.8	-41								
PT6	6/25/2017	-6.5	-47					3.6			
PT6	12/2/2017	-6.4	-46								
PT7	6/1/2016	-7.0	-46								
PT7	10/24/2016	-7.5	-54								
PT7	11/21/2017	-3.9	-34								
PT8	11/19/2016	-7.2	-52								
PT8	6/25/2017	-5.9	-42					4.5			
PT8	12/2/2017	-5.3	-39								
PT10	10/24/2016	-6.6	-46								
PT10	11/21/2017	-1.9	-25								
PT11	11/21/2017	-5.6	-43								
PT12	6/20/2016	-5.5	-44								
PT12	11/19/2016	-5.8	-42								
PT12	6/24/2017	-0.6	-22					4.2			
PT12	12/2/2017	-5.0	-37								
PZ1	07/20/13	-9.6	-55								
PZ1	05/22/16	-7.4	-53								
PZ2	03/12/16	-9.2	-66								
PZ2	05/21/16	-9.7	-65								
PZ2	08/28/16	-8.9	-61								

Sample ID	Date	$\delta^{18}O$ (‰)	δD (‰)	$\delta^{34}S_{(SO4)}$ (‰)	$\delta^{18}O_{(SO4)}$ (‰)	$\delta^{13}C$-DIC (‰) AMS	$\delta^{13}C$-DIC (‰) GEOS	Tritium (TU)	^{14}C-DIC (pMC)	Unadjusted age (years)	Adjusted age (years)
PZ2	12/18/16	-9.8	-67								
PZ3	07/20/13	-11.9	-65								
PZ3	03/12/16	-8.8	-71	7.6	3.1			1.9			
PZ3	08/28/16	-9.5	-66								
PZ3	12/18/16	-9.6	-66								
PZ4	06/08/14	-7.5	-61								
PZ4	08/15/15	-9.3	-66								
PZ4	01/31/16	-9.1	-63	10.0	26.0			<0.8			
PZ4	05/14/16	-8.7	-62	-5.2	6.3						
PZ4	08/27/16	-9.0	-63								
PZ4	12/17/16	-9.2	-65								
PZ5	06/08/14	-7.6	-59								
PZ5	03/13/16	-9.2	-62								
PZ5	05/22/16	-8.6	-60	8.1	-5.4						
PZ5	08/27/16	-8.7	-65								
PZ5	11/26/16	-7.8	-61								
PZ6	06/08/14	-7.1	-53								
PZ6	03/13/16	-8.2	-65								
PZ6	05/22/16	-8.1	-67								
PZ6	08/27/16	-9.1	-68								
PZ6	11/26/16	-8.0	-62								
PZ7	07/20/13	-10.1	-60								
PZ7	01/31/16	-8.9	-64	-1.1	5.5			<1.0			
PZ7	05/14/16	-9.3	-63								
PZ7	08/28/16	-8.3	-64								
PZ7	11/25/16	-8.4	-65								
PZ8	03/12/16	-9.8	-72	11.4	6.6			1.8			
PZ8	05/21/16	-9.4	-69								
PZ8	08/28/16	-10.2	-67								
PZ8	12/18/16	-10.9	-75								
PZ9	07/20/13	-11.0	-56								
PZ9	01/31/16	-8.4	-59	7.2	11.8						
PZ9	05/14/16	-8.1	-56								
PZ9	08/28/16	-7.8	-57								
PZ9	11/25/16	-7.5	-58								
SP1	05/19/16	-9.4	-63	9.6	9.5			0.9			

Sample ID	Date	$\delta^{18}O$ (‰)	δD (‰)	$\delta^{34}S_{(SO4)}$ (‰)	$\delta^{18}O_{(SO4)}$ (‰)	$\delta^{13}C$-DIC (‰) AMS	$\delta^{13}C$-DIC (‰) GEOS	Tritium (TU)	^{14}C-DIC (pMC)	Unadjusted age (years)	Adjusted age (years)
SP2	05/25/15	-7.9	-56								
SP2	03/12/16	-8.6	-63	36.9	7.0			1.8			
SP2	05/21/16	-7.9	-55								
SP2	08/28/16	-2.4	-24								
SP2	08/28/16	-9.1	-62								
SP2	12/18/16	-9.3	-65								
SP3	01/31/16	-8.1	-57					0.9			
SP3	05/22/16	-9.0	-61								
SP3	08/27/16	-8.7	-59								
SP3	12/17/16	-9.1	-61								
SP4	05/25/15	-5.0	-43								
SP4	08/16/15	-6.7	-52								
SP4	02/28/16	-5.9	-48	9.5	7.0			<0.5			
SP4	05/22/16	-6.7	-50								
SP4	09/25/16	-6.7	-52								
SP4	12/18/16	-6.6	-51								
SP5	02/01/14	-11.3	-61								
SP5	03/13/16	-8.4	-59	11.9	11.6			<0.5			
SP5	06/05/16	-8.4	-60								
SP5	09/02/16	-7.5	-59								
SP5	11/26/16	-7.5	-60								
SP6	02/01/14	-9.2	-55								
SP6	03/13/16	-8.0	-58					1.4			
SP6	06/05/16	-8.5	-61								
SP6	09/02/16	-7.4	-55								
SP6	11/26/16	-7.6	-61								
SP7	05/25/15	-9.8	-63								
SP7	08/15/15	-1.7	-29								
SP7	01/31/16	-9.0	-62	6.9	7.2						
SP7	05/14/16	-9.1	-62								
SP7	08/27/16	-5.9	-41								
SP7	12/17/16	-8.7	-65								
SP8	05/25/15	-7.7	-54								
SP8	02/27/16	-7.9	-55								
SP8	05/14/16	-9.1	-61								
SP8	08/27/16	-8.5	-59								

Sample ID	Date	$\delta^{18}O$ (‰)	δD (‰)	$\delta^{34}S_{(SO4)}$ (‰)	$\delta^{18}O_{(SO4)}$ (‰)	$\delta^{13}C$-DIC (‰) AMS	$\delta^{13}C$-DIC (‰) GEOS	Tritium (TU)	^{14}C-DIC (pMC)	Unadjusted age (years)	Adjusted age (years)
SP8	12/17/16	-9.1	-64								
SP9	02/27/16	-1.6	-28								
SP10	07/20/13	-10.3	-61								
SP10	10/13/13	-9.6	-55								
SP10	02/02/14	-9.4	-55								
SP10	04/19/14	-7.1	-58								
SP10	12/20/14	-8.0	-59								
SP10	03/29/15	-8.4	-59								
SP10	05/25/15	-8.5	-58								
SP10	01/31/16	-7.9	-58	14.1	13.7	-13.1	-11.1	<0.5	75.8	2300	952
SP10	05/19/16	-8.4	-58								
SP10	08/28/16	-7.5	-54								
SP10	11/25/16	-7.3	-58								
SP11	10/13/13	-9.4	-57								
SP11	03/13/16	-8.1	-54	2.8	8.7			<0.8			
SP11	06/05/16	-7.1	-55								
SP11	09/02/16	-8.4	-56								
SP11	11/26/16	-6.8	-56								
SP12	12/20/14	-8.0	-59								
SP12	02/27/16	-8.0	-59					1.2			
SP12	05/14/16	-6.5	-49								
SP12	12/17/16	-8.8	-61								
SP13	09/07/14	1.3	-7								
SP13	03/29/15	9.6	15								
SP14	03/29/15	-8.8	-58								
SP14	12/17/16	-8.6	-58								
SP15	11/11/15	-5.8	-46								
SP15	03/12/16	-7.6	-57								
SP15	12/18/16	-7.7	-59								
SP16	05/25/15	-6.5	-46								
SP16	02/28/16	-6.9	-50	14.7	7.5			<0.5			
SP16	05/22/16	-6.5	-50								
SP16	09/02/16	-6.9	-50								
SP16	12/16/16	-6.4	-51								
SP17	08/16/15	-5.3	-48								
SP17	11/11/15	-6.2	-49								

Sample ID	Date	$\delta^{18}O$ (‰)	δD (‰)	$\delta^{34}S_{(SO4)}$ (‰)	$\delta^{18}O_{(SO4)}$ (‰)	$\delta^{13}C$-DIC (‰) AMS	$\delta^{13}C$-DIC (‰) GEOS	Tritium (TU)	^{14}C-DIC (pMC)	Unadjusted age (years)	Adjusted age (years)
SP17	09/25/16	-6.9	-52								
SP17	12/16/16	-7.1	-53								
WL1	07/21/13	-11.5	-73								
WL2	06/08/14	-6.8	-58								
WL3	07/21/13	-11.1	-70								
WL3	08/03/16	-9.5	-73	6.6	9.3	-7	-10.5	<0.5	8.6	20300	18900
WL4	07/21/13	-12.4	-81								
WL5	07/20/13	-12.3	-75								
WL5	06/08/14	-9.1	-71								
WL5	08/03/16	-10.1	-79	7.4	3.5	-9.9	-7.7	<0.5	13.6	16500	15100
WL6	06/08/14	-9.8	-79								
WL7	02/01/14	-11.2	-59								
WL7	09/07/14	-7.1	-56								
WL7	12/20/14	-7.6	-58								
WL7	03/29/15	-9.8	-60								
WL7	11/11/15	-7.9	-59								
WL7	02/27/16	-8.0	-60								
WL7	05/21/16	-7.6	-57								
WL7	08/27/16	-6.4	-44								
WL7	12/16/16	-8.5	-60								
WL8	05/25/15	-11.0	-76								
WL8	08/03/16	-9.9	-77	5.0	7.6	-9.8	-6.7	<0.5	3.3	28100	26800
WL8	08/27/16	-10.4	-79								
WL9	07/20/13	-7.8	-46								
WL10	07/20/13	-10.2	-58								
WL11	07/20/13	-10.1	-60								
WL11	08/03/16	-9.4	-67	4.5		-10.8	-7.8	1.7	77.1	2150	808
WL12	05/29/16	-7.8	-53	10.7							
WL13	06/01/16	-8.6	-60	9.1	8.6	-10.5	-6.2	0.8	84.7	1370	29
WL14	05/19/16	-8.8	-62	9.7	10.7						
WL15	04/09/16	-9.8	-64	4.7	2.8			2			
WL16	05/30/16	-9.2	-64	4.8	7.3			<0.5			
WL17	05/30/16	-9.9	-67								
WL18	04/05/14	-8.4	-61	5.8			-6.3	0.8			
WL19	07/21/13	-10.3	-54								
WL19	06/08/14	-6.3	-55								

Sample ID	Date	$\delta^{18}O$ (‰)	δD (‰)	$\delta^{34}S_{(SO4)}$ (‰)	$\delta^{18}O_{(SO4)}$ (‰)	$\delta^{13}C$-DIC (‰) AMS	$\delta^{13}C$-DIC (‰) GEOS	Tritium (TU)	^{14}C-DIC (pMC)	Unadjusted age (years)	Adjusted age (years)
WL19	08/15/15	-8.6	-59								
WL20	04/05/14	-8.7	-62	5.2			-4.4	<.9 (Apparent .4)			
WL21	04/09/16	-8.7	-58	6.9	5.7						
WL22	05/29/16	-8.6	-59	5.6		-10.2	-6.4	<0.5	65.4	3510	2170
WL23	05/30/16	-10.6	-63	4.6	8.0			<0.5			
WL24	04/09/16	-8.8	-59								
WL25	05/30/16	-9.5	-57								
WL26	04/05/14	-9.4	-66	-0.9			-7.0	<0.7			
WL27	05/28/16	-7.5	-55								
WL28	04/09/16	-9.7	-58	5.0				<0.5			
WL29	05/28/16	-7.8	-58	5.3	3.5	-8.4	-5.9	<0.5	58.9	4380	3030
WL30	05/29/16	-8.4	-56								
WL31	05/20/16	-9.3	-64								
WL32	05/20/16	-9.1	-63	5.1	8.1			<0.5			
WL33	05/20/16	-9.1	-62								
WL34	05/28/16	-8.7	-59	6.6	3.1						
WL35	05/28/16	-9.3	-64								
WL36	06/01/16	-8.1	-56	5.1	4.6						
WL37	04/09/16	-9.6	-68	2.7	3.3						
WL38	05/14/16	-8.3	-60	5.9	4.8	-9.4	-7.6	<0.5	68.8	3090	1750
WL39	04/09/16	-8.6	-60		16.2			<0.5			
WL40	05/29/16	-8.0	-58		7.3			<0.5			
WL41	05/29/16	-9.3	-59	6.3	9.0						
WL42	03/26/16	-8.8	-58								
WL43	05/20/16	-8.4	-60	5.8	6.1			<0.5			
WL44	04/09/16	-9.5	-64								
WL44	05/14/16	-9.3	-62	7.0	9.0	-9.7	-8.1	<0.7	73.9	2500	1160
WL45	05/28/16	-9.1	-65								
WL46	05/30/16	-8.4	-55								
WL47	03/26/16	-8.9	-59		12.2						
WL48	05/20/16	-9.0	-64	5.8	7.6			<0.8			
WL49	05/30/16	-9.2	-60	6.5	6.9						
WL50	05/14/16	-9.0	-63	6.0	7.7						

Table 5: Water Chemistry

Sample ID	Date	Ca^{2+} (mg/L)	Mg^{2+} (mg/L)	Na^{+} (mg/L)	K^{+} (mg/L)	Sr^{2+} (ug/L)	Cl^{-} (mg/L)	SO_4^{2-} (mg/L)	Alkalinity (meq/kg)
PZ1	05/22/16						11.91	11.03	
PZ2	03/12/16	56.22	5.48	15.31	1.59	161.97	3.42	9.25	3.43
PZ2	05/21/16	54.70	5.18	15.73	1.70	160.21	4.07	12.22	3.38
PZ2	08/28/16	57.18	5.45	17.62	1.66	166.36	4.27	10.53	3.31
PZ2	12/18/16	55.46	5.15	16.36	1.66	153.27	3.95	10.20	2.16
PZ3	03/12/16	54.27	7.09	15.60	1.21	309.47	3.72	12.44	3.07
PZ3	05/21/16	59.62	7.92	18.29	1.53	340.50			
PZ3	08/28/16	60.78	7.87	18.02	1.45	342.53	4.52	12.60	3.47
PZ3	12/18/16	83.35	8.57	17.17	1.60	383.70	4.13	14.91	2.39
PZ4	06/08/14						11.23	23.20	
PZ4	08/15/15						8.73	21.60	
PZ4	01/31/16	40.64	6.29	37.24	1.41	304.55	4.78	12.42	7.09
PZ4	05/14/16	42.61	6.81	39.24	1.84	325.94	4.70	15.46	2.71
PZ4	08/27/16	45.08	6.77	39.97	1.57	320.51	4.04	11.65	3.69
PZ4	12/17/16	55.78	8.50	33.12	2.19	374.70	4.56	15.97	4.26
PZ5	06/08/14						19.87	15.00	
PZ5	03/13/16	34.05	5.71	68.14	2.56	275.18	7.51	6.07	4.71
PZ5	05/22/16	44.49	7.44	57.63	4.62	289.03	12.52	6.65	4.26
PZ5	08/27/16	41.81	6.76	58.37	3.20	280.51	7.51	6.64	4.57
PZ5	11/26/16	45.72	7.10	52.75	1.75	287.81	7.23	5.34	4.66
PZ6	06/08/14						36.59	116.44	
PZ6	03/13/16	53.07	8.76	48.02	2.87	412.04	8.43	85.47	
PZ6	05/22/16	136.88	21.06	76.71	3.76	990.45	9.33	414.06	3.65
PZ6	08/27/16	138.88	21.28	76.00	4.38	959.96	7.13	482.11	3.94
PZ6	11/26/16	182.11	28.65	88.88	5.47	1284.80	6.27	633.74	4.97
PZ7	01/31/16	66.36	6.89	14.13	0.86	347.05	4.36	25.37	3.25
PZ7	05/14/16	74.39	7.52	16.28	1.05	373.13	4.47	31.64	3.32
PZ7	08/28/16	73.33	7.85	15.12	1.07	398.74	4.19	37.88	3.85
PZ7	11/25/16	79.46	8.38	15.97	0.99	418.06	4.16	39.48	3.93
PZ8	03/12/16	73.98	14.68	34.40	1.67	502.54	10.36	10.21	5.83
PZ8	05/21/16	60.72	11.52	33.88	1.48	392.38	5.42	13.73	4.63
PZ8	08/28/16	60.60	11.50	34.31	1.54	397.49	5.80	10.50	4.54
PZ8	12/18/16	83.78	14.68	36.38	1.86	527.86	10.79	14.11	5.43
PZ9	01/31/16	73.58	12.61	25.43	1.07	413.26	13.33	15.67	4.59
PZ9	01/31/16	72.74	12.43	24.90	1.02	405.51			
PZ9	05/14/16	100.91	17.32	33.05	1.35	561.53	16.09	28.34	5.80

Sample ID	Date	Ca^{2+} (mg/L)	Mg^{2+} (mg/L)	Na^{+} (mg/L)	K^{+} (mg/L)	Sr^{2+} (ug/L)	Cl^{-} (mg/L)	SO_4^{2-} (mg/L)	Alkalinity (meq/kg)
PZ9	08/28/16	78.41	13.59	27.48	1.15	438.27	12.47	17.72	5.24
PZ9	11/25/16	74.48	13.00	27.56	1.10	422.16	9.93	14.92	5.01
SP1	05/19/16	81.68	20.99	7.10	0.85	269.41	5.69	29.75	
SP2	05/25/15						13.09	6.16	
SP2	03/12/16	98.53	28.32	137.06	9.09	596.67	11.96	10.99	11.45
SP2	05/21/16	62.52	10.45	24.92	2.04	355.18	5.34	7.81	3.26
SP2	08/28/16	76.37	9.59	36.63	9.52	314.95	7.26	7.70	5.55
SP2	08/28/16	58.79	8.10	20.13	1.65	348.78	4.74	8.83	3.86
SP2	12/18/16	154.67	31.05	236.40	6.27	707.63	32.32	79.37	18.25
SP3	01/31/16	66.57	7.59	110.05	7.28	186.52	14.89	46.45	
SP3	05/22/16	53.05	7.10	124.12	0.72	193.36	6.45	54.04	8.10
SP3	08/27/16	57.73	6.19	83.82	2.39	189.52	10.44	36.43	5.28
SP3	12/17/16	273.98	11.19	130.60	1.75	513.76	6.49	39.58	7.85
SP4	05/25/15						10.71	10.51	
SP4	02/28/16	40.93	6.14	17.15	1.52	215.39	5.74	8.50	22.45
SP4	05/22/16	62.45	7.33	18.89	1.33	294.92	6.09	10.67	
SP4	09/25/16						11.68	7.49	4.81
SP5	03/13/16	90.00	20.80	195.95	1.98	739.63	24.12	98.80	11.61
SP5	06/05/16	54.53	9.66	60.06	4.58	405.14	10.83	82.34	4.22
SP5	09/02/16	56.96	10.31	48.41	Sat'd	382.17	15.21	14.05	8.78
SP5	11/26/16	82.62	16.14	113.35	3.08	632.39	12.95	23.51	7.36
SP6	03/13/16	75.57	14.47	113.12	1.92	566.47	16.39	78.04	5.77
SP6	06/05/16	52.64	8.48	44.07	1.58	351.41	6.93	30.79	6.27
SP6	09/02/16	65.77	11.45	55.29	5.68	471.16	8.34	15.34	4.09
SP6	11/26/16	53.45	8.76	45.48	2.13	358.57	7.00	28.72	
SP7	05/25/15						8.30	12.58	
SP7	08/15/15						14.76	59.46	
SP7	01/31/16	51.25	8.77	19.24	1.97	403.62	4.59	9.68	3.13
SP7	05/14/16	62.10	10.57	22.87	2.56	502.91	4.94	11.10	3.26
SP7	08/27/16						3.64	5.44	7.98
SP7	12/17/16	94.41	12.14	23.34	2.54	614.73	4.67	12.98	3.35
SP8	05/25/15						20.09	4.84	
SP8	02/27/16	113.23	24.04	49.16	7.58	959.89	6.37	10.38	3.62
SP8	05/14/16	90.30	14.67	30.09	4.34	683.18	6.03	10.92	9.08
SP8	08/27/16	95.38	14.89	26.75	3.14	710.59	4.24	6.36	6.25
SP8	12/17/16	124.38	18.84	21.70	2.08	1012.56	4.59	9.32	1.76
SP9	02/27/16	22.82	18.70	399.89	15.10	340.31	208.60	80.74	16.08

Sample ID	Date	Ca^{2+} (mg/L)	Mg^{2+} (mg/L)	Na^{+} (mg/L)	K^{+} (mg/L)	Sr^{2+} (ug/L)	Cl^{-} (mg/L)	SO_4^{2-} (mg/L)	Alkalinity (meq/kg)
SP10	04/19/14						18.77	21.31	
SP10	12/20/14						17.29	17.09	
SP10	03/29/15						25.38	30.35	
SP10	05/25/15						19.93	20.92	
SP10	01/31/16	87.81	14.85	28.79	0.60	501.25	15.35	12.70	5.34
SP10	05/19/16	112.54	19.46	42.62	0.67	661.45	23.09	23.67	
SP10	08/28/16	91.09	23.00	48.97	0.69	709.06	20.80	15.65	8.41
SP10	11/25/16	89.76	18.45	39.22	0.52	596.25	13.51	9.94	7.10
SP11	03/13/16	76.14	17.83	84.40	3.66	493.57	14.53	122.87	6.25
SP11	06/05/16	73.08	16.68	76.84	3.92	571.07	14.99	17.86	7.93
SP11	09/02/16	75.62	19.80	79.98	1.29	667.94	16.76	14.45	9.95
SP11	11/26/16	75.76	16.42	68.56	2.35	499.62	10.90	9.39	7.18
SP12	12/20/14						24.51	44.02	
SP12	02/27/16	56.60	10.59	81.49	2.37	335.53	9.05	15.67	5.98
SP12	05/14/16	99.78	23.51	231.65	SAT'D	726.36			15.05
SP12	12/17/16	104.92	11.19	187.15	11.40	501.52	54.60	78.21	6.30
SP13	09/07/14						177.15	18.05	
SP13	03/29/15						295.36	1339.51	
SP14	03/29/15						16.24	48.64	
SP14	12/17/16	82.64	30.55	533.20	Sat'd	816.72	86.13	285.02	18.91
SP15	03/12/16	66.61	28.80	151.12	2.70	940.79	21.46	70.41	10.68
SP15	12/18/16	295.34	69.06	341.71	Sat'd	3052.39	199.23	839.38	11.41
SP16	02/28/16	58.54	10.33	42.81	3.02	402.65	8.61	21.03	4.10
SP16	05/22/16	68.73	12.39	55.01	2.95	474.29	14.90	31.67	5.05
SP16	09/02/16	12.97	6.54	36.19	0.88	177.72	20.61	21.98	4.30
SP16	12/16/16	199.60	16.75	39.56	5.45	1064.40	10.09	20.49	4.91
SP17	08/16/15						17.54	21.80	
SP17	09/25/16	54.44	8.04	28.04	1.95	324.92	7.03	14.58	4.12
SP17	12/16/16	81.48	10.73	27.29	1.97	465.39	7.14	17.87	2.40
WL2	06/08/14						11.02	13.63	
WL3	08/03/16	25.92	0.23	160.18	1.13	69.32	21.12	403.62	-0.28
WL5	08/03/16	1.72	0.19	70.67	0.71	7.65	6.74	12.67	2.09
WL7	09/07/14						15.84	14.61	
WL7	12/20/14						8.84	11.37	
WL7	02/27/16	45.21	6.87	31.61	1.37	351.47	5.07	10.67	3.49
WL7	05/21/16	37.86	6.80	30.74	1.39	340.61	5.41	12.97	3.28
WL7	08/27/16	37.52	4.07	13.90	3.80	236.16	3.96	9.11	2.45

Sample ID	Date	Ca^{2+} (mg/L)	Mg^{2+} (mg/L)	Na^{+} (mg/L)	K^{+} (mg/L)	Sr^{2+} (ug/L)	Cl^{-} (mg/L)	SO_4^{2-} (mg/L)	Alkalinity (meq/kg)
WL7	12/16/16	42.12	6.51	28.49	1.34	333.53	5.72	13.65	1.81
WL8	08/03/16	12.67	0.44	63.46	1.18	126.71	3.93	38.85	1.86
WL8	08/27/16	12.95	0.43	63.25	1.20	125.58	4.05	37.74	2.33
WL11	08/03/16	38.06	4.59	7.14	0.75	168.85	3.61	11.81	1.91
WL12	05/29/16	51.93	7.87	16.72	1.23	158.71	15.61	6.33	2.90
WL13	06/01/16	83.43	14.40	10.47	1.18	339.95	9.43	29.46	4.09
WL14	05/19/16	80.42	16.08	7.62	1.05	447.96	6.83	25.35	4.25
WL15	04/09/16	56.85	6.13	8.11	0.80	205.92	9.90	19.13	1.24
WL16	05/30/16	28.02	2.05	19.34	0.96	237.82	3.43	9.11	1.26
WL17	05/30/16	25.11	2.45	14.40	0.78	134.46	3.58	6.59	1.29
WL18	04/05/14	50.70	6.44	13.04	1.16	187.71	7.05	6.88	3.56
WL19	06/08/14						10.35	18.71	
WL19	08/15/15						9.93	5.21	
WL20	04/05/14	52.17	6.56	12.58	1.07	156.15	8.98	7.11	3.43
WL21	04/09/16	48.24	5.89	11.77	1.04	158.21	8.56	8.68	2.63
WL22	05/29/16	53.75	6.40	11.01	1.12	162.12	6.91	10.36	2.09
WL23	05/30/16	28.32	1.53	24.07	0.94	315.97	3.63	20.55	1.38
WL24	04/09/16	49.93	4.70	14.04	0.92	109.23	10.75	11.60	2.09
WL25	05/30/16	43.88	6.98	11.11	0.95	199.67	4.89	8.93	2.07
WL26	04/05/14	47.08	6.18	40.66	1.36	343.01	6.42	79.55	3.11
WL27	05/28/16	48.56	6.99	12.90	0.97	123.77	7.39	8.36	2.35
WL28	04/09/16	49.97	7.53	15.58	1.12	310.12	16.55	7.71	2.45
WL29	05/28/16	48.95	6.76	12.87	1.04	143.69	11.35	9.28	1.75
WL30	05/29/16	51.42	7.75	15.97	1.15	148.57	16.12	7.51	3.39
WL31	05/20/16	43.42	4.39	9.47	0.74	102.36	4.75	8.85	2.74
WL32	05/20/16	31.93	2.02	22.80	0.95	371.83	3.76	13.92	2.44
WL33	05/20/16	50.92	4.10	9.89	0.84	111.75	7.64	15.68	2.21
WL34	05/28/16	48.41	6.56	10.83	1.01	125.60	9.57	8.03	2.61
WL35	05/28/16	26.51	1.57	22.16	1.07	300.84	3.68	15.71	2.50
WL36	06/01/16	50.20	6.91	14.46	1.10	144.63	8.95	13.66	2.56
WL37	04/09/16	57.29	4.60	8.18	0.76	203.87	4.07	11.95	2.91
WL38	05/14/16	96.17	10.96	25.78	1.39	305.40	18.64	65.20	4.42
WL39	04/09/16	47.51	7.24	15.40	1.17	132.41	8.03	6.20	2.89
WL40	05/29/16	50.04	7.23	13.77	1.05	243.70	10.64	8.47	2.81
WL41	05/29/16	20.82	1.08	46.90	1.09	161.34	4.24	19.03	1.52
WL42	03/26/16	50.61	7.27	13.43	1.00	143.22	10.69	10.65	2.36
WL43	05/20/16	46.04	7.82	18.20	1.13	375.67	9.03	11.21	2.77

Sample ID	Date	Ca^{2+} (mg/L)	Mg^{2+} (mg/L)	Na^{+} (mg/L)	K^{+} (mg/L)	Sr^{2+} (ug/L)	Cl^{-} (mg/L)	SO_4^{2-} (mg/L)	Alkalinity (meq/kg)
WL44	04/09/16	51.20	4.96	9.73	0.77	128.35	5.04	8.87	2.49
WL44	05/14/16	50.63	4.97	9.78	0.77	128.52	5.15	8.84	2.70
WL45	05/28/16	22.76	1.87	16.63	0.75	172.75	3.50	8.88	1.30
WL46	05/30/16	48.62	6.20	10.06	0.97	144.74	7.54	7.76	2.38
WL47	03/26/16	50.66	5.28	10.89	1.06	171.08	10.74	10.49	2.68
WL48	05/20/16	31.22	2.30	17.31	0.89	336.83	3.73	16.51	1.49
WL49	05/30/16	53.04	6.93	12.44	1.15	174.66	9.95	15.57	3.00
WL50	05/14/16	9.22	0.21	60.37	0.85	67.70	3.87	23.09	2.26

APPENDIX A: SUPPLEMENTARY DATA

Table A1: Locations

Sample ID	Data Source	Sample Type	Latitude (Decimal Degrees)	Longitude (Decimal Degrees)	Altitude (m)	Well Depth (m)	Screened Interval (m)
CV1	Truebe et al. (2016)	Cave	31.75000	-110.75000	1603		
CV2	UA	Cave					
PZ10	DBG[1]	piezometer	31.58485	-110.49951	1447		
SP18	HMI[2]	spring	31.82727	-110.68560	1435		
SP19	HMI	spring	31.88160	-110.71101	1456		
SP20	HMI	spring	31.80882	-110.76135	1610		
SP21	HMI	spring	31.78773	-110.63860	1390		
SP22	HMI	spring	31.86790	-110.77784	1396		
SP23	HMI	spring	31.84431	-110.74473	1523		
SP24	HMI	spring	31.84852	-110.74921	1551		
SP25	HMI	spring	31.88734	-110.71191	1504		
SP26	HMI	spring	31.87652	-110.71982	1471		
SP27	HMI	spring	31.83380	-110.68853	1404		
SP28	HMI	spring	31.82792	-110.73755	1509		
SP29	HMI	spring	31.82694	-110.78608			
SP30	HMI	spring	31.88261	-110.76148			
SP31	RFCD/PAG[3]	spring	31.98490	-110.64781	1073		
SP32	RFCD/PAG	spring	31.98490	-110.64781	1073		
SP33	SIA[4]	spring	31.68946	-110.83883	2339		
SP34	SIA	spring	31.89340	-110.71511	1537		
CC1	ADWR[5]	well	31.72863	-110.60804	1413		
CC2	ADWR	well	31.75596	-110.61216	1388		
CC3	ADWR	well	31.78481	-110.60157	1370		
CC5	ADWR	well	31.80109	-110.59659	1351		
CC6	ADWR	well	31.81378	-110.59085	1324		
GC2	ADWR	well	31.72112	-110.72010	1512		
GC14	ADWR	well	31.75582	-110.61848	1387		
GC15	ADWR	well	31.75596	-110.61216	1388		
GC16	ADWR	well	31.77001	-110.57184	1376		
WL51	DBG	well	31.57652	-110.49919	1458		
WL52	DBG	well	31.58916	-110.50649	1451		
WL53	Gu et al. (2005)	well					
WL54	Gu et al. (2005)	well					
WL55	Gu et al. (2005)	well					
WL56	Gu et al. (2005)	well					
WL57	Gu et al. (2005)	well					
WL58	Gu et al. (2005)	well					
WL59	HMI	well	31.77566	-110.72347	1530		
WL60	HMI	well	31.77825	-110.74342	1582		

[1] DBG Desert Botanical Garden
[2] HMI Hudbay Minerals Inc.
[3] RFCD/ PAG Regional Flood Control District/ Pima Association of Governments
[4] SIA Sky Island Alliance
[5] ADWR Arizona Department of Water Resources

Sample ID	Data Source	Sample Type	Latitude (Decimal Degrees)	Longitude (Decimal Degrees)	Altitude (m)	Well Depth (m)	Screened Interval (m)
WL61	HMI	well	31.82025	-110.73772			
WL62	HMI	well	31.81652	-110.76739			
WL63	HMI	well	31.81643	-110.76738			
WL64	HMI	well	31.81470	-110.74075			
WL65	HMI	well	31.81473	-110.74085			
WL66	HMI	well	31.83478	-110.73783			
WL67	HMI	well	31.83485	-110.73776			
WL68	HMI	well	31.83487	-110.73771			
WL69	HMI	well	31.85177	-110.72999			
WL70	HMI	well	31.85171	-110.73005			
WL71	HMI	well	31.84689	-110.74965			
WL72	HMI	well	31.84682	-110.74960			
WL73	HMI	well	31.84403	-110.73642		1000	244-975
WL74	HMI	well	31.83441	-110.75147			
WL75	HMI	well	31.83749	-110.74905			
WL76	HMI	well	31.84093	-110.75487			
WL77	HMI	well	31.83739	-110.76046			
WL78	HMI	well	31.82969	-110.76405			
WL79	HMI	well	31.83522	-110.73106			
WL80	HMI	well	31.84689	-110.70976			
WL81	HMI	well	31.84697	-110.70977			
WL82	HMI	well	31.84706	-110.70975			
WL83	HMI	well	31.83007	-110.72178			
WL84	HMI	well	31.83015	-110.72173			
WL85	HMI	well	31.82320	-110.73070			
WL86	HMI	well	31.82312	-110.73072			
WL87	HMI	well	31.80610	-110.75304			
WL88	HMI	well	31.86484	-110.69555			
WL89	HMI	well	31.85234	-110.67682			
WL90	HMI	well	31.83266	-110.69126			
WL91	HMI	well	31.86162	-110.69577			
WL92	HMI	well	31.90076	-110.66372			
WL93	RFCD/PAG	well	31.98435	-110.65027	1113		
WL94	RFCD/PAG	well	32.03399	-110.67593	988		
WL95	RFCD/PAG	well	31.99592	-110.57783	1080		

Table A2: Field Parameters

Sample ID	Data Source	Date	Dissolved Oxygen (%)	Specific conductance (µs/cm)	TDS	pH	Temp (°C)
CV1	Cave						19.8
SP32	spring	6/4/2002		726.6		7.93	20.4
SP32	spring	8/2/2002		723.3		7.88	28.0
SP32	spring	5/8/2003		778.3		7.39	17.8
SP32	spring	9/3/2008		609.5	415.0	7.93	30.6
SP32	spring	9/22/2009		885.7	612.4	7.99	23.2
SP32	spring	9/21/2010		704.0	471.7	7.32	23.7
SP32	spring	9/7/2011		975.1	663.0	7.31	27.0
SP32	spring	9/10/2012	68	574.1	367.3	7.63	23.9
SP32	spring	11/20/2012	44	693.0	450.0	7.35	20.4
SP32	spring	2/24/2012*		719.6	490.6	7.60	15.9
WL53	well	09/18/98				7.67	
WL53	well	09/24/99				6.91	
WL54	well	06/23/99				7.04	
WL54	well	04/05/01				7.07	
WL54	well	11/14/03				7.05	
WL55	well	10/06/98				4.49	
WL55	well	01/14/99				4.60	
WL56	well	07/16/99				6.80	
WL56	well	03/29/01				7.14	
WL56	well	11/06/02				7.14	
WL56	well	12/05/03				7.40	
WL57	well	10/08/98				7.19	
WL57	well	03/29/01				7.17	
WL57	well	12/05/03				7.70	
WL58	well	09/24/99				7.00	
WL93	well	05/27/14		902.7	621.7	7.54	15.9
WL93	well	02/20/15		710.0	474.5	7.84	23.3
WL95	well	05/20/14			50.0		
WL95	well	10/07/14			50.0		

Table A3: Isotopes

Sample ID	Date	$\delta^{18}O$ (‰)	δD (‰)	$\delta^{34}S_{(SO4)}$ (‰)	$\delta^{18}O_{(SO4)}$ (‰)	$\delta^{13}C$-DIC (‰) GEOS	^{14}C-DIC (pMC)	Tritium (TU)
CV1	11/25/2017			4.30	0.20			1.8
CV2	11/24/2017			3.90	insuff.			3.5
PZ10	11/11/15	-6.9	-52					
SP18	04/19/10	-6.7	-50					
SP19	05/04/10	-7.8	-58					
SP19	01/04/11	-8.0	-59					
SP20	04/29/08	-9.0	-62					
SP20	07/29/08	-8.7	-63				-10.7	3.6
SP20	10/21/08	-8.6	-61					
SP20	05/03/10	-8.6	-61					
SP20	06/22/10	-8.5	-60					
SP20	05/25/11	-8.6	-62					
SP20	09/01/11	-8.5	-62					
SP20	12/06/11	-7.8	-58					
SP20	03/26/12	-7.8	-58					
SP20	08/28/12	-8.2	-60					
SP20	11/29/12	-6.8	-53			94.8	-7.0	
SP20	11/13/13	-6.3	-54			93.2	-6.2	
SP20	12/06/11	-7.7	-58					
SP20	11/29/12	-6.6	-53			94.6	-6.9	
SP20	11/13/13	-6.3	-52			93.1	-6.1	
SP21	04/06/12	-8.2	-59					
SP21	06/18/14	-8.4	-60				-10.2	
SP21	06/18/14	-8.5	-60				-9.9	
SP22	05/06/10	-8.5	-61					
SP22	06/28/10	-8.4	-61					
SP22	01/03/11	-8.3	-60					
SP22	05/31/11	-8.4	-61					
SP22	09/09/11	-8.2	-62					
SP22	12/05/11	-8.5	-61					
SP22	03/27/12	-8.5	-60					
SP22	08/30/12	-8.4	-57					
SP22	11/27/12	-8.4	-59			68.3	-9.0	
SP22	11/18/13	-8.2	-59			90.1	-12.1	
SP22	03/27/12	-8.4	-62					
SP23	07/23/08	-9.3	-70				-12.0	5.3
SP23	10/29/08	-8.4	-60					
SP23	09/01/11	-8.2	-61					
SP23	08/28/12	-5.6	-48					
SP24	04/22/08	-8.1	-61					
SP24	07/23/08	-8.9	-62				-12.0	1.9
SP24	10/29/08	-8.6	-61					
SP24	05/03/10	-8.5	-60					
SP24	06/23/10	-8.5	-60					
SP24	12/01/11	-8.3	-59					
SP24	03/26/12	-8.2	-59					
SP24	08/28/12	-8.2	-57					
SP25	11/12/13	-8.5	-62			82.9	-9.9	
SP26	05/04/10	-6.7	-53					

Sample ID	Date	$\delta^{18}O$ (‰)	δD (‰)	$\delta^{34}S_{(SO4)}$ (‰)	$\delta^{18}O_{(SO4)}$ (‰)	$\delta^{13}C$-DIC (‰) GEOS	^{14}C-DIC (pMC)	Tritium (TU)
SP26	11/30/11	-7.2	-56					
SP26	03/26/12	-6.8	-51					
SP27	04/23/08	-10.3	-75					
SP27	07/29/08	-9.5	-73				-8.0	<0.6
SP27	10/21/08	-10.0	-77					
SP27	04/19/10	-10.5	-78					
SP27	05/25/11	-10.4	-79					
SP27	09/01/11	-10.4	-79					
SP27	12/01/11	-10.5	-79					
SP27	03/26/12	-10.4	-77					
SP27	08/28/12	-10.0	-75					
SP27	11/30/12	-10.5	-78			16.4	-8.2	
SP27	11/13/13	-10.2	-76			15.1	-8.7	
SP28	04/23/08	-6.6	-54					
SP28	07/29/08	-7.2	-54				-9.0	1.2
SP28	10/21/08	-7.9	-56					
SP28	04/14/10	-7.2	-56					
SP28	06/22/10	-7.3	-56					
SP28	12/05/11	-7.6	-56					
SP28	03/26/12	-7.4	-57					
SP28	11/28/12	-8.1	-57			70.1	-10.3	
SP28	11/13/13	-8.0	-59			72.5	-10.3	
SP29	10/27/08	-7.4	-55					
SP30	07/30/08	-8.4	-65					5.1
SP30	10/21/08	-8.4	-60					
SP30	05/06/10	-8.5	-60					
SP30	06/30/10	-8.3	-60					
SP30	01/07/11	-8.2	-59					
SP30	06/03/11	-7.1	-55					
SP30	09/12/11	-6.7	-47					
SP30	12/09/11	-8.3	-59					
SP30	03/29/12	-8.3	-61					
SP30	08/31/12	-8.3	-61					
SP30	12/06/12	-7.4	-54			88.5	-17.6	
SP30	07/30/08	-8.4	-65				-11.0	4.8
SP31	06/04/02	-7.2	-51					
SP31	08/02/02	-7.2	-51					
SP31	05/08/03	-6.9	-49					
SP31	09/30/14	-8.5	-60					
SP32	9/30/2014	-8.5	-60					
SP33	11/15/2014	-9.2	-63					
SP34	11/14/2015	-8.3	-59					
WL51	06/04/15	-6.1	-50					
WL51	08/15/15	-6.3	-53					
WL51	10/10/15	-6.8	-53					
WL51	06/04/16	-6.9	-51					
WL52	06/21/15	-8.8	-73					
WL53	09/18/98	-10.5	-73					<1
WL53	09/24/99	-9.2	-72	1.7	3.4			
WL54	06/23/99	-8.8	-59	11.7	10.5			2.3
WL54	04/05/01	-9.1	-63	13.3	12.2			4.6

Sample ID	Date	$\delta^{18}O$ (‰)	δD (‰)	$\delta^{34}S_{(SO4)}$ (‰)	$\delta^{18}O_{(SO4)}$ (‰)	$\delta^{13}C$-DIC (‰) GEOS	^{14}C-DIC (pMC)	Tritium (TU)
WL54	11/14/03	-8.2	-59	13.8	13.7			1.3
WL55	10/06/98	-8.3	-60					<1
WL55	01/14/99	-8.3	-58					
WL56	07/16/99	-9.0	-64	10.8	10.8			2.2
WL56	03/29/01	-8.6	-61	-0.4	5.6			2.6
WL56	11/06/02	-8.2	-59	6.9	9.8			3.5
WL56	12/05/03	-8.2	-58	12.6	12.8			1.3
WL57	10/08/98	-8.8	-63					2.0
WL57	03/29/01	-8.8	-62	10.3	10.7			1.8
WL57	12/05/03	-8.4	-60	11.5	12.8			1.4
WL58	09/24/99	-8.3	-61	-6.8	2.6			
WL59	04/25/08	-7.3	-57					
WL59	04/25/08	-7.2	-58					
WL60	04/25/08	-9.1	-65					
WL61	07/01/13	-8.5	-60			16.1	-10.0	
WL62	08/19/08	-8.8	-63					
WL63	08/15/08	-8.8	-62				-13.5	<0.7
WL63	11/29/08	-8.8	-60					
WL63	12/182008	-8.8	-61					
WL64	07/03/08	-8.1	-60					0.7
WL65	07/08/08	-10.9	-76				-8.2	1.2
WL66	09/11/08	-8.7	-61					
WL67	09/04/08	-9.0	-63					
WL68	09/02/08	-10.7	-76					
WL69	07/22/08	-7.7	-56					0.9
WL69	04/13/11	-7.3	-57					
WL69	07/27/11	-7.3	-59					
WL69	02/16/12	-7.4	-58					
WL69	08/01/12	-7.4	-56					
WL69	10/17/12	-7.5	-56			66.4	-8.5	
WL69	10/23/13	-7.4	-58			66	-9.5	
WL70	07/17/08	-8.6	-65					1.3
WL71	06/18/08	-8.9	-63				-11.3	1.5
WL71	11/29/08	-8.8	-62					
WL71	12/18/08	-8.8	-62					
WL72	06/24/08	-10.0	-69				-12.8	2.2
WL73	04/21/08	-10.5	-74					
WL73	10/29/08	-10.6	-74					
WL74	04/22/08	-9.2	-65					
WL74	11/06/14	-8.9	-62					
WL75	10/21/08	-8.9	-62					
WL75	11/29/08	-8.9	-61					
WL75	12/18/08	-8.9	-62					
WL75	10/23/08	-9.6	-67					
WL75	10/21/08	-8.8	-62					
WL76	10/14/08	-9.1	-64					
WL76	10/16/08	-9.1	-64					
WL76	10/12/08	-9.0	-64					
WL76	10/13/08	-9.1	-64					
WL77	10/02/08	-9.6	-67					
WL77	10/07/08	-10.4	-75					

Sample ID	Date	$\delta^{18}O$ (‰)	δD (‰)	$\delta^{34}S_{(SO4)}$ (‰)	$\delta^{18}O_{(SO4)}$ (‰)	$\delta^{13}C$-DIC (‰) GEOS	^{14}C-DIC (pMC)	Tritium (TU)
WL77	10/03/08	-9.7	-68					
WL77	10/04/08	-9.9	-70					
WL78	09/27/08	-8.9	-62					
WL78	09/23/08	-8.9	-62					
WL78	09/25/08	-8.9	-62					
WL78	11/06/14	-8.9	-62					
WL79	04/24/13	-10.5	-75			2.2	-10.9	
WL79	04/29/08	-10.7	-77					
WL80	08/28/08	-12.4	-95					
WL81	08/26/08	-8.1	-60					
WL81	08/26/09	-8.1	-61					
WL81	10/28/09	-8.3	-61					
WL81	12/14/09	-8.1	-61					
WL81	02/19/10	-8.1	-59					
WL81	05/27/10	-8.3	-61					
WL81	08/18/10	-8.4	-60					
WL81	11/29/10	-8.3	-60					
WL81	04/14/11	-8.2	-60					
WL81	07/27/11	-8.2	-61					
WL81	02/27/12	-8.3	-61					
WL81	08/07/12	-8.4	-58					
WL81	10/17/12	-8.2	-60			87	-7.4	
WL81	10/23/13	-8.3	-61			44.3	-7.1	
WL82	08/22/08	-9.3	-72					
WL82	08/26/09	-9.4	-74					
WL82	10/28/09	-9.8	-74					
WL82	12/14/09	-9.5	-74					
WL82	02/19/10	-9.7	-72					
WL82	05/27/10	-9.7	-73					
WL82	08/18/10	-9.8	-73					
WL82	11/29/10	-9.7	-73					
WL82	04/14/11	-9.5	-72					
WL82	07/27/11	-9.5	-73					
WL82	02/27/12	-9.5	-73					
WL82	08/07/12	-9.5	-71					
WL82	10/23/13	-9.4	-71			16.9	-8.9	
WL82	10/23/13	-9.5	-70			14.5	-9.6	
WL82	11/29/10	-9.6	-72					
WL82	04/14/11	-9.5	-72					
WL83	07/15/08	-7.0	-55				-8.4	1.7
WL83	08/24/09	-6.7	-56					
WL83	10/27/09	-6.8	-56					
WL83	12/11/09	-6.8	-57					
WL83	02/18/10	-6.8	-55					
WL83	05/28/10	-7.0	-56					
WL83	11/29/10	-7.2	-56					
WL83	04/20/11	-6.8	-56					
WL83	02/28/12	-6.9	-51					
WL83	08/07/12	-6.9	-54					
WL83	10/18/12	-7.0	-53			76.2	-6.8	
WL83	10/22/13	-6.8	-55			73.6	-8.2	

Sample ID	Date	$\delta^{18}O$ (‰)	δD (‰)	$\delta^{34}S_{(SO4)}$ (‰)	$\delta^{18}O_{(SO4)}$ (‰)	$\delta^{13}C$-DIC (‰) GEOS	^{14}C-DIC (pMC)	Tritium (TU)
WL83	08/24/09	-6.8	-57					
WL84	07/12/08	-7.9	-60				-9.0	0.6
WL84	11/29/08	-7.9	-60					
WL84	12/18/08	-7.9	-61					
WL84	08/25/09	-7.6	-61					
WL84	10/27/09	-7.8	-62					
WL84	12/11/09	-7.7	-62					
WL84	02/18/10	-7.7	-60					
WL84	05/28/10	-7.9	-61					
WL84	08/18/10	-7.9	-61					
WL84	12/01/10	-7.9	-61					
WL84	04/20/11	-7.8	-60					
WL84	02/28/12	-7.8	-61					
WL84	08/07/12	-7.9	-60					
WL84	10/18/12	-7.9	-60			24.6	-7.6	
WL84	10/22/13	-8.0	-61			20.5	-8.1	
WL85	07/01/08	-7.4	-54				-7.8	0.7
WL85	08/27/09	-7.4	-58					
WL85	10/23/09	-7.1	-58					
WL85	12/10/09	-7.4	-59					
WL85	02/17/10	-7.6	-57					
WL85	05/25/10	-7.5	-59					
WL85	12/01/10	-7.6	-58					
WL85	04/18/11	-7.3	-56					
WL85	02/28/12	-7.5	-58					
WL85	08/07/12	-7.5	-56					
WL85	10/18/12	-7.7	-56			82.6	-4.8	
WL85	10/28/13	-7.4	-57			80.1	-7.3	
WL85	10/23/09	-7.3	-59					
WL85	05/25/10	-7.6	-58					
WL85	10/28/13	-7.5	-58			79.5	-7.1	
WL86	06/26/08	-10.2	-71				-9.4	1.0
WL86	08/27/09	-10.0	-76					
WL86	10/29/09	-10.4	-75					
WL86	12/11/09	-10.3	-77					
WL86	02/18/10	-10.4	-75					
WL86	05/26/10	-10.4	-76					
WL86	08/17/10	-10.4	-77					
WL86	11/30/10	-10.6	-76					
WL86	04/15/11	-10.3	-75					
WL86	02/15/12	-10.2	-75					
WL86	07/31/12	-10.2	-73					
WL86	10/16/12	-10.1	-74			8	-6.8	
WL86	10/29/13	-10.4	-73			1.2	-7.5	
WL86	08/17/10	-10.4	-76					
WL86	02/15/12	-10.2	-76					
WL86	07/31/12	-10.3	-74					
WL86	10/16/12	-10.1	-73			8.3	-7.0	
WL87	07/24/08	-8.3	-61					0.6
WL87	10/29/09	-8.4	-62					
WL87	12/09/09	-8.2	-62					

Sample ID	Date	$\delta^{18}O$ (‰)	δD (‰)	$\delta^{34}S_{(SO4)}$ (‰)	$\delta^{18}O_{(SO4)}$ (‰)	$\delta^{13}C$-DIC (‰) GEOS	^{14}C-DIC (pMC)	Tritium (TU)
WL87	02/17/10	-8.5	-62					
WL87	05/27/10	-8.4	-62					
WL87	12/01/10	-8.1	-62					
WL87	04/19/11	-8.0	-60					
WL87	02/27/12	-8.2	-62					
WL87	08/07/12	-8.3	-60					
WL87	10/17/12	-8.2	-57			63.3	-7.3	
WL87	10/22/13	-8.3	-60			86.1	-7.9	
WL87	12/09/09	-8.3	-63					
WL87	02/17/10	-8.4	-62					
WL88	07/29/08	-7.6	-57					3.4
WL88	11/29/08	-7.7	-56					
WL88	12/18/08	-7.6	-56					
WL89	08/07/08	-6.9	-54					0.6
WL90	08/13/08	-10.6	-78					<1
WL91	10/30/13	-6.6	-52			52.7	-9.4	
WL92	11/04/13	-7.7	-58			50	-17.9	
WL93	05/27/14	-8.8	-68					
WL93	09/15/14	-8.3	-64					
WL93	02/18/15	-8.0	-61					
WL93	06/24/15	-7.7	-61	9.2			-6.6	0.5
WL94	06/25/99	-8.1	-56					
WL95	05/20/14	-8.3	-60					
WL95	10/07/14	-8.4	-58					
WL95	02/18/15	-8.3	-60					
WL95	06/24/15	-8.1	-58	13.0			-10.2	1.2

Table A4: Water Chemistry

Sample ID	Date	Ca^{2+} (mg/L)	Mg^{2+} (mg/L)	Na^{+} (mg/L)	K^{+} (mg/L)	Sr^{2+} (ug/L)	Cl^{-} (mg/L)	SO_4^{2-} (mg/L)	Alkalinity (mg/L)	Alkalinity (meq/kg)
CV1	11/25/2017	71.00	42.38	5.90	0.56	96.12			354.51	
CV2	11/24/2017	66.47	3.63	1.89	0.42	111.76			220.27	
SP18	04/19/10						13.00	51.00		
SP19	05/04/10						16.00	18.00		
SP19	01/04/11						21.90	71.00		
SP31	08/02/02						150-200	200.00		
SP31	05/08/03						1.00	1.00		
SP31	03/03/17	125.43	24.14	38.95	2.34	935.07				6.12
SP32	6/4/2002	81.00	21.00	48.00	< 5.0		17.00	79.00		
SP32	8/2/2002	87.00	20.00	50.00	< 5.0		15.00	91.00		
SP32	5/8/2003	99.00	25.00	44.00	< 5.0		15.00	84.00		
SP32	9/3/2008	86.00	14.00	28.00	5.40		6.50	42.00		
SP32	9/22/2009	120.00	26.00	44.00	3.20		13.00	120.00		
SP32	9/21/2010	90.00	17.00	39.00	3.20		7.20	59.00		
SP32	9/10/2012	98.00	18.00	25.00	2.10		4.40	46.00		
SP32	11/20/2012	100.00	18.00	25.00	2.20		4.50	43.00		
SP32	9/30/2014	87.00	15.00	20.00	2.60		2.60	30.00		
SP32	2/24/2012*	86.00	20.00	33.00	2.40		6.20	70.00		
WL51	06/04/15	68.30	11.75	19.29	1.63	530.71	20.61	14.28		
WL51	08/15/15						20.88	13.70		
WL51	06/04/16						14.08	10.57		5.60
WL52	06/21/15						14.36	13.25		
WL53	09/18/98	102.00		144.00			7.00	520.00	78	
WL53	09/24/99	116.00					10.00	372.00		
WL54	06/23/99	176.00		11.00			6.00	295.00		
WL54	04/05/01	138.00		12.00				300.00		

Sample ID	Date	Ca^{2+} (mg/L)	Mg^{2+} (mg/L)	Na^{+} (mg/L)	K^{+} (mg/L)	Sr^{2+} (ug/L)	Cl^{-} (mg/L)	SO_4^{2-} (mg/L)	Alkalinity (mg/L)	Alkalinity (meq/kg)
WL54	11/14/03	154.00		14.00			6.00	307.00	205	
WL55	10/06/98	67.00		43.00			10.00	397.00		
WL55	01/14/99	69.00		58.00			27.00	404.00		
WL56	07/16/99	141.00		13.00			7.00	216.00		
WL56	03/29/01	144.00		18.00			8.00	228.00		
WL56	11/06/02	148.00		18.00			8.00	252.00	185	
WL57	10/08/98	141.00		16.00			6.00	269.00	225	
WL57	03/29/01	155.00		15.00			7.00	222.00		
WL57	12/05/03							256.00		
WL58	09/24/99	188.00		27.00			9.00	413.00		
WL91	10/30/13						13.00	59.00		
WL93	09/15/14	59.00	37.00	110.00			41.00	51.00		< 6.0
WL93	02/20/15	30.00	31.00	91.00			43.00	43.00		< 6.0
WL93	06/24/15	37.00	36.00	93.00	7.60			42.00		
WL95	10/07/14	150.00	35.00	39.00	3.40		9.10	360.00	250	
WL95	02/18/15	150.00	34.00	40.00	3.60		8.20	330.00	270	
WL95	06/24/15	160.00	38.00	40.00	3.70		8.60	390.00		

REFERENCES

Ajami, H. 2009. Quantifying spatial and temporal variability of mountain system recharge and riparian evapotranspiration in semi-arid catchments. University of Arizona, PhD dissertation 496 p.

Anderson, S. R. 1987. Cenozoic stratigraphy and geologic history of the Tucson Basin, Pima County, Arizona. U.S. Geological Survey Water-Resources Investigations Report 87-4190, 23 p.

Arizona Water Atlas. 2003. Arizona Department of Water Resources (ADWR). Volume 3, Section 3.3 Cienega Creek. 36 p.

Baillie, M. N., Hogan, J. F., Ekwurzel, B., Wahi, A. K., & Eastoe, C. J. 2007. Quantifying water sources to a semiarid riparian ecosystem, San Pedro River, Arizona. Journal of Geophysical Research: Biogeosciences, 112(3), 1–13p.

Beier, P., Majka, D., and Bayless, T. 2007. Arizona missing linkages: Rincon-Santa Rita-Whetstone linkage design. Report to Game and Fish Department. School of Forestry, Northern Arizona University. 189 p.

Bittson, A.G. 1976. Analysis of gravity data from Cienega Creek area, Pima and Santa Cruz Counties, Arizona. University of Arizona, M.S. thesis 92 p.

Boggs, J. M. 1980. Impact of future ground-water development in Cienega Creek area, Pima, Santa Cruz and Cochise Counties. University of Arizona, M.S. thesis. 145 p.

Brod Jr., L.G., 2005. Geology of selected areas, Sawmill Canyon Fault zone, northeast Santa Cruz county, Arizona. Arizona Geological Survey Contributed report CR-11-D, 65 p.

Clark, I. and Fritz, P. 1997. Environmental Isotopes in Hydrogeology. CRC Press, ISBN 9781566102492- CAT#L1249, 342 p.

Coes, A., and Pool, D. 2007. Ephemeral-stream channel and basin-floor infiltration and recharge in the Sierra Vista subwatershed of the upper San Pedro Basin, southeastern Arizona. U.S. Geological Survey Professional Paper 1703-J, 253-311 p.

Cohee, G. V, Bates, R.G., Wright, W. B. 1976. Changes in stratigraphic nomenclature by the U.S. Geological Survey, 1975. U.S. Geological Survey Bulletin 1294–A, 64 p.

Craig, H. 1957. Isotopic Standards for Carbon and Oxygen and Correction Factors for Mass Spectrometric Analysis of Carbon Dioxide. Geochimica et Cosmochimica Acta. 12. 133-149. 10.1016/0016-7037(57)90024-8.

Drewes, H. 1968. New and revised stratigraphic names in the Santa Rita Mountains of southeastern Arizona. U.S. Geological Survey Bulletin 1274-C, 19 p.

Drewes, H. 1971. Mesozoic stratigraphy of the Santa Rita Mountains, southeast of Tucson, Arizona. U.S. Geological Survey Professional Paper 658-C, 87 p.

Drewes, H. 1972. Structural geology of the Santa Rita Mountains, southeast of Tucson, Arizona. U.S. Geological Survey Professional Paper 748, 35 p. and Plate 1

Drewes, H. 1973. Geochemical reconnaissance of the Santa Rita Mountains southeast of Tucson, Arizona. U.S. Geological Survey Bulletin 1365, 74 p.

Drewes, H. 1981. Tectonics of southeastern Arizona. U.S. Geological Survey Professional Paper, 1144, 101 p.

Eastoe, C. J., Gu, A., and Long, A. 2004. The origins, ages and flow paths of groundwater in Tucson Basin: Results of a study of multiple isotope systems. Groundwater Recharge in a Desert Environment: The Southwestern United States, 9, 217–234 p.

Eastoe, C.J., Watts, C.J., Ploughe, M., and Wright, W.E. 2011. Future use of tritium in mapping Pre-Bomb groundwater volumes. Groundwater, Vol. 50., No. 1, Jan-Feb 2012, 87-93 p.

Eastoe, C.J., Hess, G. and Mahieux, S., 2014, Identifying recharge from tropical cyclonic storms, Baja California Sur, Mexico, Ground Water, doi 10.1111/gwat.12183

Eastoe, C. J. 2016. Stable O, H Isotopes In Tucson Rain Associated With Hurricanes and Tropical Depressions, 2013-2016. Addendum to Eastoe, C.J., Hess, G. and Mahieux, S., 2014, Identifying recharge from tropical cyclonic storms, Baja California Sur, Mexico, Ground Water, doi 10.1111/gwat.12183

Eastoe, C.J. and Towne, D., 2018. Regional zonation of groundwater recharge mechanisms in alluvial basins of Arizona: Interpretation of isotope mapping. Journal of Geochemical Exploration, in press.

Federal Register. 2014. Endangered and threatened wildlife and plants; determination of threatened status for the western distinct population segment of the Yellow-billed Cuckoo (Coccyzus americanus). Fish and Wildlife Service, Department of the Interior. Vol. 70, No. 192. 48 p.

Garfin, G., Franco, G., Blanco, H., Comrie, A., Gonzalez, P., Piechota, Smith, R., and Waskom R. 2014. Southwest climate change impacts in the United States: The Third National Climate Assessment. J.M. Melillo, T.C. Richmond and G.W. Yohe, Eds., U.S. Global Change Research Program, 462–486 p.

Geraghty and Miller. 1970. Ground-water report Empire Ranch property Pima and Santa Cruz counties, Arizona. Geraghty and Miller, Inc. No. 60, 33 p.

Glenn, E.P., Scott, R.L., Nguyen, U., Nagler, P.L., 2015. Wide-area ratios of evapotranspiration to precipitation in monsoon-dependent semiarid vegetation communities. J. Arid Envir. 117, 84-95.

Gu, A. 2005. Sable isotope geochemistry of sulfate in groundwater of southern Arizona: Implications for groundwater flow, sulfate sources, and environmental significance. University of Arizona, PhD dissertation 256 p.

Gu, A., Gray, F., Eastoe, C. J., Norman, L. M., Duarte, O., and Long, A. 2008. Tracing ground water input to base flow using sulfate (S, O) isotopes. Ground Water, 46(3), 502–509 p.

Harshbarger, J.W., and Assoc. 1974. Potential water development on Empire Ranch lands. Harshbarger and Assoc. and Associates preliminary draft, 7 p.

Harshbarger J.W., and Assoc. 1975. Analysis of Ground Water Development Program in the Empire Ranch Area. Harshbarger and Associates preliminary draft, 80 p.

Hopkins, C. B., McIntosh, J. C., Eastoe, C., Dickinson, J. E., and Meixner, T. 2014. Evaluation of the importance of clay confining units on groundwater flow in alluvial basins using solute and isotope tracers: the case of Middle San Pedro Basin in southeastern Arizona (USA). Hydrogeology Journal, 22(4), 829–849 p.

Huth, H.J. 1996. Hydrogeochemical modeling of western mountain front recharge, Upper Cienega Creek sub-basin, Pima County, Arizona. University of Arizona, M.S. thesis 120 p.

Jasechko, S., and Taylor, R. G. 2015. Intensive rainfall recharges tropical groundwaters. Environmental Research Letters, 10(2015) 124015, 8 p.

McClaran, M.P. and Van Devender, T.R. 1995. The Desert Grassland; Desert Grassland History: Changing Climates, Evolution, Biogeography, and community dynamics. The University of Arizona Press, Tucson. 1995. Book, 346 p.

Meixner, T., Manning, A. H., Stonestrom, D. A., Allen, D. M., Ajami, H., Blasch, K. W., Brookfield, A.E., Castro, C.L., Clark, J.F., Gochis, D.J., Flint, A.L., Neff, K.L., Niraula, R., Rodell, M., Scanlon, B.R., Singha, K., and Walvoord, M. A. 2016. Implications of projected climate change for groundwater recharge in the western United States. Journal of Hydrology, 534, 124–138 p.

Osterkamp, W.R. 1973. Ground-water recharge in the Tucson area, Arizona. U.S. Geological Survey Map I-844-E, 1:250,000.

Pima Association of Governments (PAG). 2005. Unique water nomination for Davidson Canyon Draft. Regional Flood Control District watershed planning report, 63 p.

Pima Association of Governments (PAG). 2000. Lower Cienega Basin source water study prepared by Pima Association of Governments for Pima County, 33 p.

Pima County. (2011). Cienega Creek, 2011(January 31). Retrieved from www.pima.gov/nrpr/apps/permits.htm

Phillips, F. M., Hogan, J. F., and Scanlon, B. R. 2004. Introduction and overview. Groundwater Recharge in a Desert Environment: The Southwestern United States, AGU 9, 1–14 p.

Rosemont Copper Company. 2012. Integrated watershed summary; the Rosemont project. Rosemont Copper Company report. 177 p.

Schrader, F.C. 1915. Mineral deposits of the Santa Rita and Patagonia mountains Arizona. U.S. Geological Survey Bulletin 582. 373 p.

Stonestrom, D. A., Constantz, J., Ferré, T. P. A., and Leake, S. A. 2007. Ground-Water recharge in the arid and semiarid southwestern. U.S. Geological Survey Professional Paper 1703, 1–11 p.

Tillman, F. D., Cordova, J. T., Leake, S. A., Thomas, B. E., and Callegary, J. B. 2011. Water availability and use pilot: methods development for a regional assessment of groundwater availability, southwest alluvial basins, Arizona. U.S. Geological Survey Scientific Investigations Report 2011-5071, 132 p.

Final Environmental Impact Statement (FEIS). 2013. FEIS for the Rosemont Copper Project; A proposed mining operation Coronado National Forest Pima County, Arizona. United States Department of Agriculture, MB-R3-05-6e, 496 p.

Wagner, J.D.M., Cole, J.E., Beck, J.W., Patchett, P.J., Henderson, G.M., Barnett, H.R., 2010. Moisture variability in the southwestern United States linked to abrupt glacial climate change. Nat. Geosci. 3, 110–113

Wahi, A. K., Hogan, J. F., Ekwurzel, B., Baillie, M. N., and Eastoe, C. J. 2008. Geochemical quantification of semiarid mountain recharge. Ground Water, 46(3), 414–425 p.

Wright, W.E.,2001. δD and $\delta^{18}O$ in mixed conifer systems in the U.S. Southwest: The potential of $\delta^{18}O$ in *Pinus ponderosa* tree rings as a natural environmental recorder. University of Arizona, Tucson, Arizona, Unpub. Ph.D. Diss., 328 p.